Cuadernos de Investigación Geográfica *Geographical Research Letters*	2026	Nº 52 (1)	pp. 99-129	EISSN 1697-9540

http://doi.org/10.18172/cig.7072

LANDSCAPE DYNAMICS OF MARLY SLOPES IN THE LOWER VALLEY OF WADI TAMRI (MOROCCO): AN INTEGRATED APPROACH USING GEOMORPHOMETRY, TOPOSEQUENCES, AND REMOTE SENSING

HICHAM IRIFI*, ABDELLATIF TRIBAK

MNADSS – School of Geography Sidi Mohamed Ben Abdellah University Fez-Saïs, 30000 Fez, Morocco.

ABSTRACT. The mountainous marly slopes of the Atlantic High Atlas host a unique, vulnerable ecosystem shaped by a complex interplay of biotic, abiotic, and human (anthropogenic) factors. Characterized by steep slopes, poor soils, and degraded Argan (*Argania spinosa*) forests, this landscape exhibits active and complex geomorphological processes, with the presence of diverse erosion forms (gullies and rills) indicating ongoing instability. The study focused on the dynamics of marly slopes in the lower valley of Wadi Tamri in the northern part of Agadir Ida Ou Tanane province. Using geomorphometric analysis, remote sensing, and field observations, we investigated the impact of various factors, including climate, geology, and human activities, on landscape evolution. Various applied geomorphometric indices were compared with the results of a hydrological evaluation model. The comparison was made using two digital elevation models with multiple dates (2007 and 2014). To assess land use changes within this sparsely forested, marly slope landscape unit, Landsat imagery from 1984, 2000 and 2022 was analyzed, supported by landscape point sampling and field validation to facilitate interpretation of the maximum likelihood classification algorithm. The results showed that the number, length, drainage and hydrographic density values of gullies decreased between 2007 and 2014. Bifurcation and length ratios vary according to stream order and demonstrate some evolution during this period. Evolutionary stages and scenarios are marked by the degradation of the forested landscape between 1984 and 2022. Conversely, the area of marly substrate within the landscape unit has increased by 891.30 ha between 2000 and 2022. Declining forest cover can expose marly surfaces to hydric erosion. This research provides a scientific foundation for further investigation of marly slopes and offers valuable insights that will serve as an example for regional soil and water conservation strategies.

Dinámica del paisaje de las laderas margosas en el valle inferior del wadi Tamri (Marruecos): un enfoque integrado mediante geomorfometría, toposecuencias y teledetección

RESUMEN. Las vertientes montañosas y margosas del Alto Atlas Atlántico albergan un ecosistema único y vulnerable, configurado por una compleja interacción de factores bióticos, abióticos y antrópicos. Caracterizado por pendientes pronunciadas, suelos someros y formaciones degradadas de *Argania spinosa*, este paisaje manifiesta procesos geomorfológicos activos, donde la presencia de diversas incisiones erosivas (cárcavas y surcos) evidencia una inestabilidad morfodinámica continua. El estudio se centró en la dinámica de las vertientes margosas del valle inferior del wadi Tamri, situado en el sector septentrional de la provincia de Agadir Ida-Outanane. Mediante el uso de parámetros geomorfométricos, teledetección y prospecciones de campo, se investigó la incidencia de diversos factores-climáticos, litológicos y antrópicos en la evolución del paisaje. Asimismo, se contrastaron los índices geomorfométricos aplicados con los resultados obtenidos de un modelo de simulación hidrológica. El análisis comparativo se basó en el uso de Modelos Digitales de Elevaciones (MDE) multitemporales (2007 y 2014). Para evaluar la dinámica de los usos del suelo en esta unidad paisajística –caracterizada por vertientes margosas y una cobertura forestal exigua–, se procesaron imágenes Landsat correspondientes a los años 1984, 2000 y 2022. Este proceso se complementó con muestreos representativos y validaciones in situ, destinados a optimizar la precisión del algoritmo de clasificación por máxima verosimilitud (Maximum Likelihood Classification). Los resultados indican que el número, la longitud y la densidad de drenaje de las incisiones erosivas disminuyeron entre 2007 y 2014. Asimismo, las relaciones de bifurcación y longitud variaron según el orden de los canales, evidenciando una evolución morfológica durante dicho periodo. Estos escenarios evolutivos están estrechamente vinculados a la degradación del paisaje forestal registrada entre 1984 y 2022. Por el contrario, la superficie de afloramientos margosos dentro de la unidad paisajística se incrementó en 891,30 ha entre 2000 y 2022. La pérdida de cobertura forestal deja el sustrato margoso vulnerable a la erosión hídrica superficial. Esta investigación constituye una base científica para el estudio de vertientes inestables y aporta información clave para el diseño de estrategias regionales de conservación de suelos y gestión del agua.

Key words: Landscape evolution, soil erosion, gullying, land use change, geomorphometry, toposequence, remote sensing.

Palabras clave: evolución del paisaje, erosión del suelo, cárcavas, cambio en el uso del suelo, geomorfometría, toposecuencia, teledetección.

Received: 13 October 2025

Accepted: 1 February 2026

***Corresponding author:** Hicham Irifi, MNADSS–School of Geography Sidi Mohamed Ben Abdellah University Fez-Saïs, 30000 Fez. E-mail: Hicham.irifi@usmba.ac.ma

1. Introduction

Marly slopes in The Atlantic High Atlas Mountains are highly dynamic, exhibiting various forms of erosion and surface obstructions that significantly transform the mountainous landscape. This landscape results from the interaction of numerous biotic, abiotic, and anthropogenic factors and component (Irifi, 2023). The marly slopes are heavily impacted by gullying erosion, widely regarded as one of the most significant soil loss processes in the region. As with many other Mediterranean areas, the region is highly susceptible to water hydric erosion (García-Ruiz *et al.*, 2013). This vulnerability arises from steep slopes, fragile soils, and harsh autumn climate conditions, which follow a long, dry summer season that significantly reduces vegetation cover (El Khalili *et al.*, 2013; Tribak, 2020; Tribak *et al.*, 2021). Many research papers have demonstrated the evaluation erosion impact on soil loss in Morocco through diverse methods and approaches, such as RUSLE (Amhani and Tribak, 2022; El Aroussi, 2013; Tribak *et al.*, 2021), GIS and machine learning (Aouragh *et al.*, 2023; Bammou *et al.*, 2024; Hitouri *et al.*, 2024), Statistics methods (Meliho *et al.*, 2018), and field measurements. In fact, ephemeral gully erosion, a type of soil erosion prevalent on steep and average slopes in the Moroccan mountains, is a significant problems by progressively reducing cultivable land and soil quality (García-Ruiz *et al.*, 2013).

Indeed, the study of ephemeral gully erosion has benefited greatly from advancements in remote sensing technology, including high-resolution satellite imagery and DEM processing (Aouragh *et al.*, 2023; Dai *et al.*, 2019; Liu *et al.*, 2024). The application of these tools has primarily focused on mapping and identifying ephemeral gullies (Peter *et al.*, 2014; Sheshukov *et al.*, 2018; Yang *et al.*, 2017), generating land use maps (El Garouani *et al.*, 2009), assessing soil erosion vulnerability (Evans and Lindsay, 2010; Tribak *et al.*, 2021), and overlaying multiple influencing factors to understand their combined effect. Studying ephemeral gullies is important because it provides insight into their evolution and the forces that drive them. Accurate prediction of advancement rates is essential for the implementation of effective erosion control measures (Liu *et al.*, 2024). Automatic identification of ephemeral gullies using DEM analysis is a promising method for detecting spatial heterogeneity and dynamics. This approach has been employed in numerous hydrological and geomorphological studies (Benzougagh *et al.*, 2019; Farhan *et al.*, 2015; Grecu *et al.*, 2007; Irifi and Tribak, 2024b; Paulinus *et al.*, 2016). This research area still presents a notable constraint due to a restricted diachronic analysis and an underutilization of geomorphometry and remote sensing to document the development and modification dynamics of gullies. Quantifying the evolution of gullies using multi-date DEMs and analyzing physical parameters provides a deeper understanding of the geomorphological evolution of a gully network, from first to last order according to Strahler's classification (Strahler, 1957). The diversity and complexity of driving forces influencing gully dynamics require geomorphological and statistical analyses of all the gullies on the scale of the marly slopes, which are strongly affected by gullying processes. In this context, toposequences serve as a valuable tool for deciphering the complex and diverse controlling factors that drive the vulnerability of marly slopes to water erosion (Alves *et al.*, 2024; Catani *et al.*, 2010). Toposequences conducted between 2020 and 2022, are opting for a global analysis with the aim of detecting the driving forces.

The lower valley of Wadi Tamri is characterized by a highly dynamic and ever-changing slope landscape under the degraded cover of *Argania spinosa* and *Tetraclinis articulata* (Irifi, 2023; Irifi and Tribak, 2024a,b). The Moroccan territory, is currently experiencing its most prolonged dry spell in recent history, with significantly reduced precipitation and a notable rise in temperatures (Bannari *et al.*, 2017). The intense morphogenic activity that characterizes the slopes of the lower Wadi Tamri valley can largely be attributed to the friable nature of its Hauterivian marly formations. This susceptibility to weathering and erosion manifests in spectacular forms of erosion, ablation and accumulation, especially on the middle and lower slope sections where thick colluvium has accumulated (Irifi and Tribak, 2024b). The combined effects of climate change, induced drought, poor land management, and human activity have intensified soil erosion and slope instability. These processes transform the landscape from minor erosional forms into deep gullies, limiting ecological and agricultural productivity (Bousba *et al.*, 2024). The prevalence of marly formations and the need to protect local infrastructure make this area a key site for studying erosion and promoting sustainable land management. Integrating soil conservation into local and regional policies is essential to effectively combat land degradation (Bousba *et al.*, 2024).

By combining multi-source data with field observations, we conduct an integrated analysis to understand how hydrographic networks evolve within slope dynamics. This approach allows us to quantify the impacts of land use and rainfall variability on different stream orders. Furthermore, field toposequences reveal the complex interactions between biotic, abiotic, and human factors that guide slope processes, addressing a significant gap in previous research. Studying the landscape of these marl slopes is a relevant approach to understanding their functioning and evolutionary dynamics. It can also help diagnose the risk of soil erosion in the region. This study has four main objectives: 1) modelling the relationships between numerical indices and geomorphometry from DEM analysis, combining with fieldwork carried out between 2020 and 2022, in order to develop different toposequences and to validate the results of image processing and the derived data on land use ; 2) The methodology involves explaining gullying processes and their evolution through field-based toposequences and statistical analysis, assessing land-use changes via remote sensing, and evaluating the evolution of climatic conditions over time. 3) developing a scientific basis for the lower Tamri valley that can inform decision-making and serve as a model for broader application, and 4) proposing a straightforward landscape project centered on two primary management axes: edaphic and forest resources.

2. Study area

The study area is part of the lower valley of the wadi Tamri basin in the central part of the Atlantic High Atlas. Its geomorphological and bioclimatic conditions have given rise to the diverse and characteristic landscapes of this region (Irifi *et al.*, 2020; Irifi and Tribak, 2024a) (Fig. 1). It is bordered by the Igouzolen basin to the north, the wadi Tamraght basin to the south, the Argana corridor to the east and the Atlantic Ocean to the west. The wadi Tamri basin covers an area of 2,391 km², with ground altitudes ranging from 1,270 meters on the highest peaks to 10 meters in the lowlands (Irifi, 2023; Irifi *et al.*, 2020).

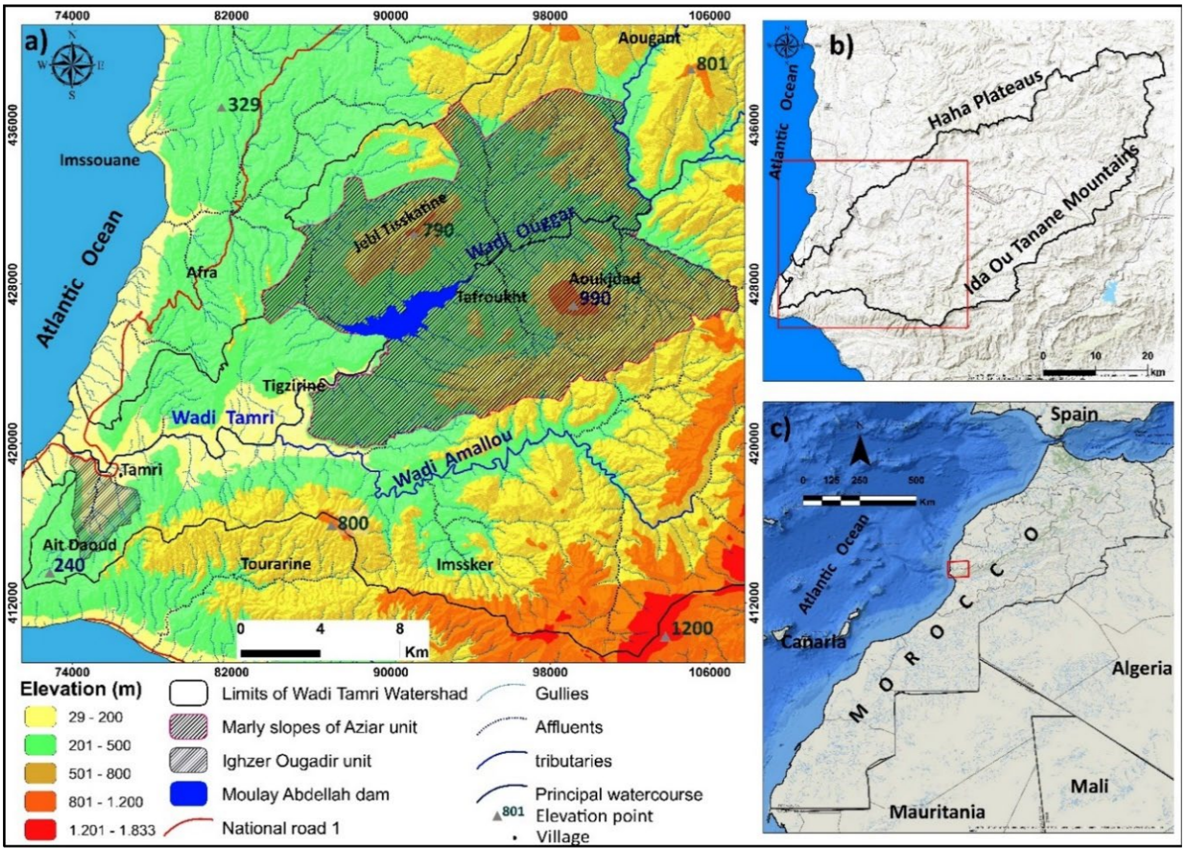

Figure 1. Location of the study area: a) Lower valley of wadi Tamri, b) Map of the wadi Tamri basin, c) Location of the Study Area in Morocco.

The study area is situated within the Essaouira-Agadir sedimentary basin, characterized by diverse Mesozoic rocks (Jurassic carbonates, Cretaceous marls) (Adams, 1979; Ambroggi, 1963; Charton *et al.*, 2021; Weisrock, 1980) and Quaternary deposits. Exposed along the Anklout and Imouzzer anticlines are Early to Late Jurassic limestone and dolomite deposits, which are significantly affected by karstic processes (Ambroggi, 1963; Charton *et al.*, 2021; Weisrock, 1980, 1985). Overlying these are Cretaceous formations, primarily composed of marly units (Hauterivian, Aptian, Albian) interbedded with limestones and sandstones (Adams, 1979; Ambroggi, 1963; Charton *et al.*, 2021). The key finding related to erosion is that differential erosion affecting these easily erodible marls and clays has directly led to widespread slope instability (Farhan *et al.*, 2015). The study focused on two landscape units within the lower Wadi Tamri valley-the large Aziar unit (232.91 km²) and the smaller Ighzer Ougadir basin (10.16 km²). These units, ranging from 200 to 900 meters in elevation, share a dissected relief with declining slopes. Crucially, both are dominated by Cretaceous marly lithological formations (soft rocks), whose widespread presence is identified as the key factor causing slope instability and soil erosion (Farhan *et al.*, 2015) (Fig. 2). In general, the lithological characteristics of the study sites are highly conducive to differential and selective erosion. This vulnerability explains the opening of the landscape and the predominance of various structural landforms, such as cuestas, chevrons, and combes, within the lower valley of the wadi Tamri.

The climate is semi-arid Mediterranean (Peel *et al.*, 2007). Rainfall is concentrated irregularly during the winter months. Annual averages range from 300 mm on the Tamri plateau (356 m) to 500 mm in the Imouzzer (1310 m) and Ain Assmama (1580 m) mountains. In the Tamri and Imouzzer stations, the average maximum temperature is 28°C, while the minimum is 9°C, with summer temperatures reaching 35°C (El Ouahidi, 2008; Irifi, 2023; Irifi *et al.*, 2020). Winter rainfall peaks are conducive to progressive incisions resulting in the continuous formation of deep gullies. Their transverse and longitudinal profiles also feature irregularities, combined with steep slopes, low vegetation cover and fragile substrate, resulting in a dissected landscape. The study area possesses rich floristic diversity, featuring several endemic species, notably the Argan tree (*Argania spinosa*) and Thuya (*Tetraclinis articulata*) (Emberger, 1925; Irifi *et al.*, 2020; Irifi and Tribak, 2024a). The Argan tree, which dominates at lower altitudes (10 to 540 m) in the infra-Mediterranean stage, is experiencing a continuous decline due to overexploitation and poor regeneration rates dependent on environmental and human factors (Irifi and Tribak, 2024a). Conversely, Thuya thrives at higher elevations (above 550 m) in the thermo-Mediterranean stage, often associated with species like *Genista tricuspidata* and *Pistacia lentiscus* (Emberger, 1925; Irifi, 2023; Irifi *et al.*, 2020; Irifi and Tribak, 2024a).

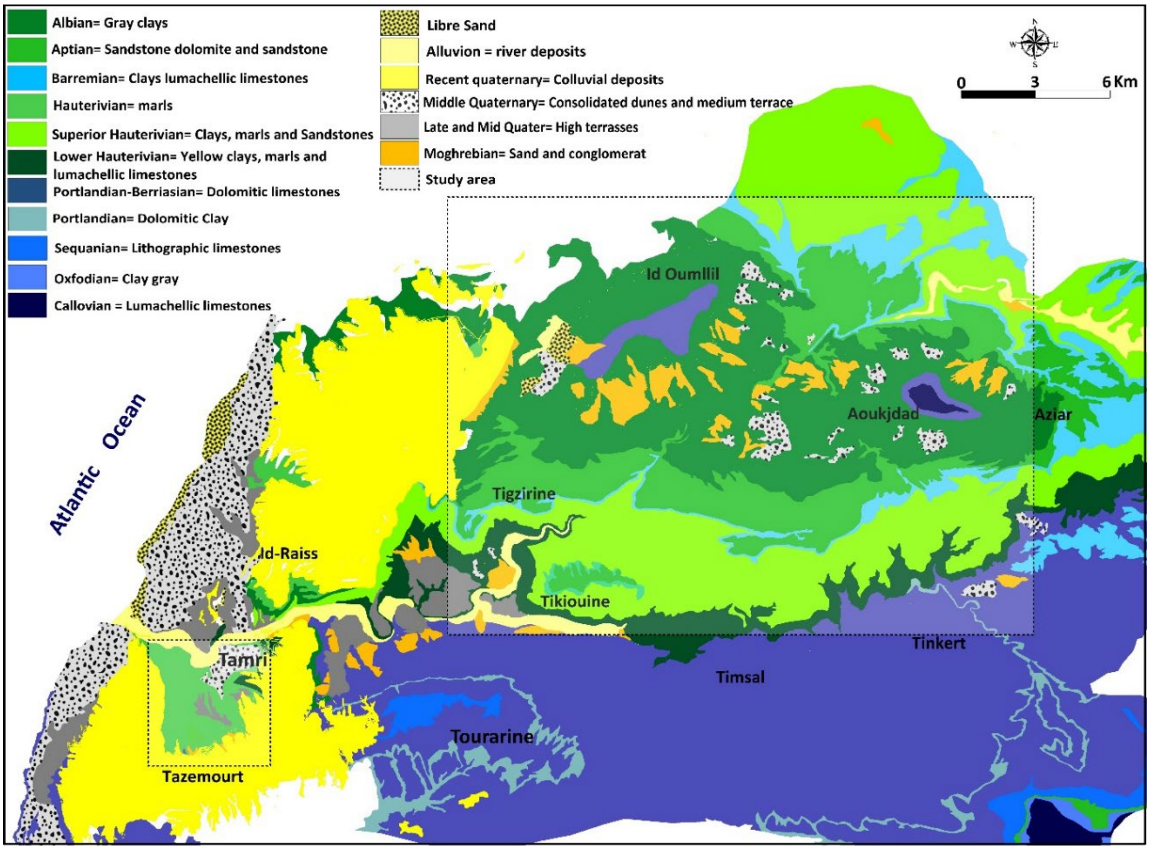

Figure 2. Geological and lithological characteristics of the lower valley of wadi Tamri. Source: Geological map of Taghazout 1/100000 (1971).

3. Material and Methods

This article emphasizes the integration of geomorphometry, toposequences, and remote sensing analysis in the lower valley of Wadi Tamri, illustrating the geomorphological evolution of marly slopes under degraded vegetation cover (Benzougagh *et al.*, 2019; Farhan *et al.*, 2015; Grecu *et al.*, 2007; Irifi and Tribak, 2024b; Srinivasa Vittala *et al.*, 2004; Vijith and Satheesh, 2006). Comparing different sample sites under varying natural conditions such as land use, soil structures, and vegetation cover in the two sampling units, allows for studying site-specific factors and broader mapping of land use changes through satellite image processing. This also facilitates the quantification of gully development in terms of number and length.

3.1. Data Source and preprocessing

The dataset used in this study is diverse and complementary, as shown in (Table 1). The hydrographical and topographical parameters were analyzed using DEMs from 2007 and 2014 with ArcGIS software. The DEMs were derived from the Advanced Land Observing Satellite (ALOS-

PALSAR) conducted in 2007 and the Shuttle Radar Topography Mission (SRTM) conducted in 2014. The datasets were downloaded from the U.S. Geological Survey (USGS) and the Alaska Satellite Facility (ASF) platforms (https://earthexplorer.usgs.gov/), (https://search.asf.alaska.edu/#/?dataset=ALOS). The DEM data was obtained with a resolution of 30 × 30 m. We selected the 2007 DEM due to its comparable accuracy to the most recent 2014 DEM, representing the latest digital elevation model. It enabled the study of various natural parameters (hypsometric analysis, slopes, exposure, relief, topographic wetness index, sediment transport index, Stream Power Index, etc.). Also, it permits the automatic extraction of the hydrographical networks within the study area using the Hydrology tool in the Spatial Analyst Tools of ArcGIS software. The process of automated stream delineation followed a sequence of steps: starting with the fill operation, then progressing through flow direction, flow accumulation, condition tool, stream ordering, and vectorization of the stream order network (Pareta and Pareta, 2012; Srinivasa Vittala *et al.*, 2004). This facilitated the calculation of numbers, lengths, hydrographic density, drainage density, confluence ratio (bifurcation) and length ratio (Benzougagh *et al.*, 2019; Farhan *et al.*, 2015; Irifi and Tribak, 2024b; Srinivasa Vittala *et al.*, 2004; Vijith and Satheesh, 2006).

Table 1. Types of data used.

Type of data	Date	Resolution	Type of treatment	Data source
Satellite images		30 * 30 m	Supervised classification	https://earthexplorer.usgs.gov
Landsat 5 TM	08/1984			
Landsat 7 ETM+	08/2000			
Landsat 8 OLI-TIRS	09/2022			
DEMs	2007 and 2014	30*30 m	Hydrographical and topographical analysis	https://search.asf.alaska.edu/#/?dataset=ALOS
SAS.planete-*Satellite* Google Earth	2022	21 m	Landscape representation and Visual analysis	SAS.planete
Climate Data	1981-2022		Standardized Precipitation Index	https://power.larc.nasa.gov/data-access-viewer/

A 30-meter DEM can effectively identify larger, well-defined gullies and analyze their landscape-scale dynamics. However, its suitability is contingent on gully size, architecture, and complexity. Substantial gullies (several meters wide and deep) are typically visible as slope breaks and elevation changes (Hayakawa and Oguchi, 2006). At a broader level, this resolution allows for valuable analysis of gully network density, orientation, and connectivity within our catchments (Culler *et al.*, 1961). Conversely, a 30 m DEM may struggle to represent or detect ephemeral or small, recent gullies (under a few meters wide or deep) (Chen *et al.*, 2024). Consequently, fine-scale morphological features like head cuts and detailed channel variations will be weakly captured or absent, limiting in-depth morphometric analysis (Dai *et al.*, 2020). Furthermore, in very steep terrain, this resolution may not accurately reflect the micro-topography crucial for understanding gully initiation and development (Cui *et al.*, 2024; Dewitte *et al.*, 2015; Zare *et al.*, 2022). We addressed this by decreasing the "condition" or an equivalent SQL expression within Arc Toolbox as part of our hydrographic network analysis process. This parameter acts as a threshold that determines which cells or accumulated flow values are considered part of the hydrographic network. By significantly decreasing this threshold value (to less than 1000), we emphasize areas with lower accumulated flow.

To achieve a finer scale of hydrographic network analysis, the study intentionally decreased the flow accumulation threshold in the DEM processing. This methodological adjustment ensures that smaller, ephemeral gullies-which naturally have low catchment areas and thus low flow accumulation values-are retained and included in the analysis, alongside the larger, higher-order streams (Castillo *et* *al.*, 2014; Chen *et al.*, 2024; Grecu *et al.*, 2007). This approach allows for the identification of both persistent and ephemeral drainage features, enabling a more comprehensive understanding of gully evolution, as higher-order streams often originate from these smaller features. After converting the raster hydrographic network into a vector file of gullies, the study utilized Strahler's ordering system to classify each stream (Ciccolini *et al.*, 2024; Dai *et al.*, 2020). This step was crucial for quantifying gully characteristics, allowing researchers to determine the length and number distributions for each hierarchical order, which are essential parameters for analyzing gully morphology, erosion processes, and land degradation dynamics (Ciccolini *et al.*, 2024, Strahler, 1952a, 1957) (Fig. 3).

The study used 30-meter resolution Landsat satellite images (from 1984, 2000, and 2022) as the primary data source. To ensure accurate interpretation, the images underwent geometric correction, band compositing, and pan-sharpening. Land use/land cover data for the two sampling units were then derived through supervised classification using the 'maximum likelihood' algorithm in ArcGIS software (Table 1 and Fig. 4). The analysis categorized the landscape into three structures: Argan forest cover, marl substrate and cultivated silty-clayey soils (Irifi, 2023). Homogeneity of appearance is a key element in characterizing and delimiting the overall landscape into distinct landscape structures (Irifi, 2023). The choice of these classes is based on information points and samples derived from recognizing landscape elements and structures. Validation is ensured through transects and sample plots in the field, as well as by using images from Google Earth Pro and Statistical validation was performed by calculating the Kappa Coefficient and Overall Accuracy (Table 8).

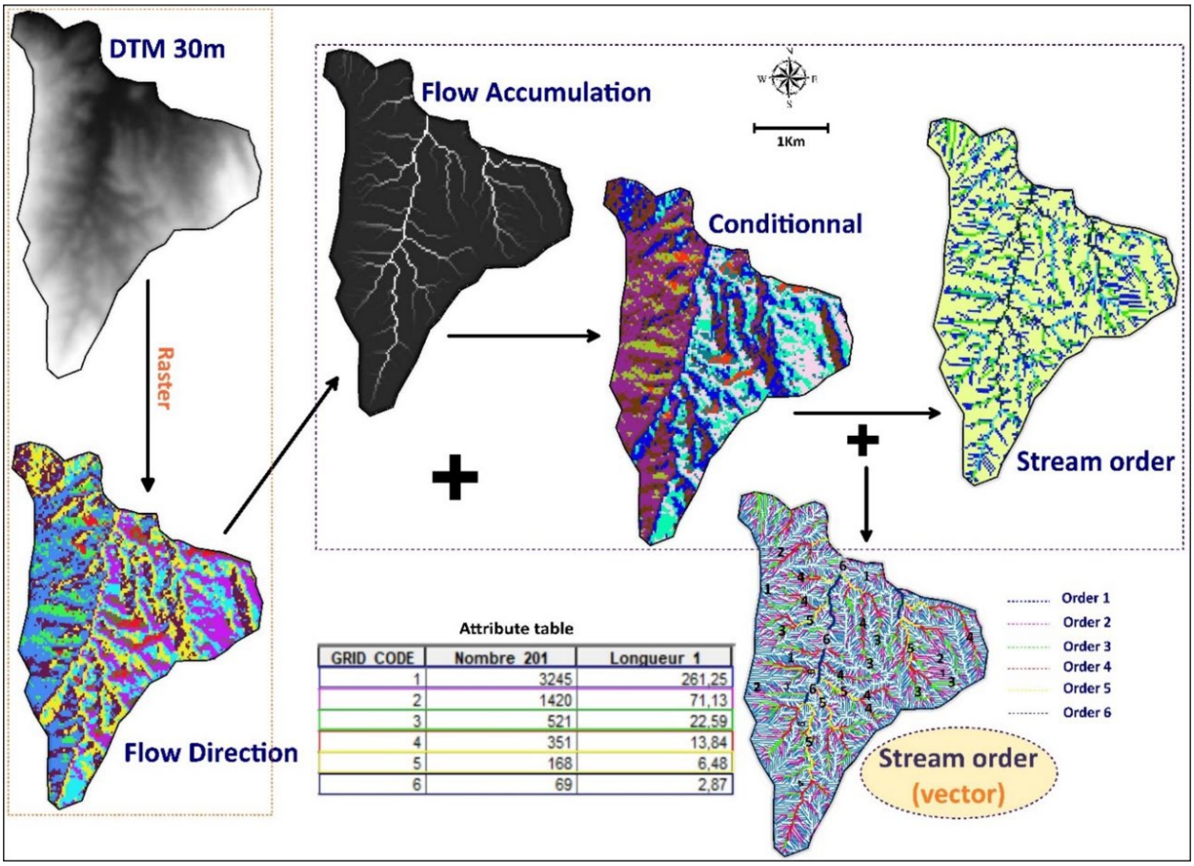

Figure 3. Stream order reconstruction in the Ighzer Ougadir catchment using a 30 m resolution DEM.

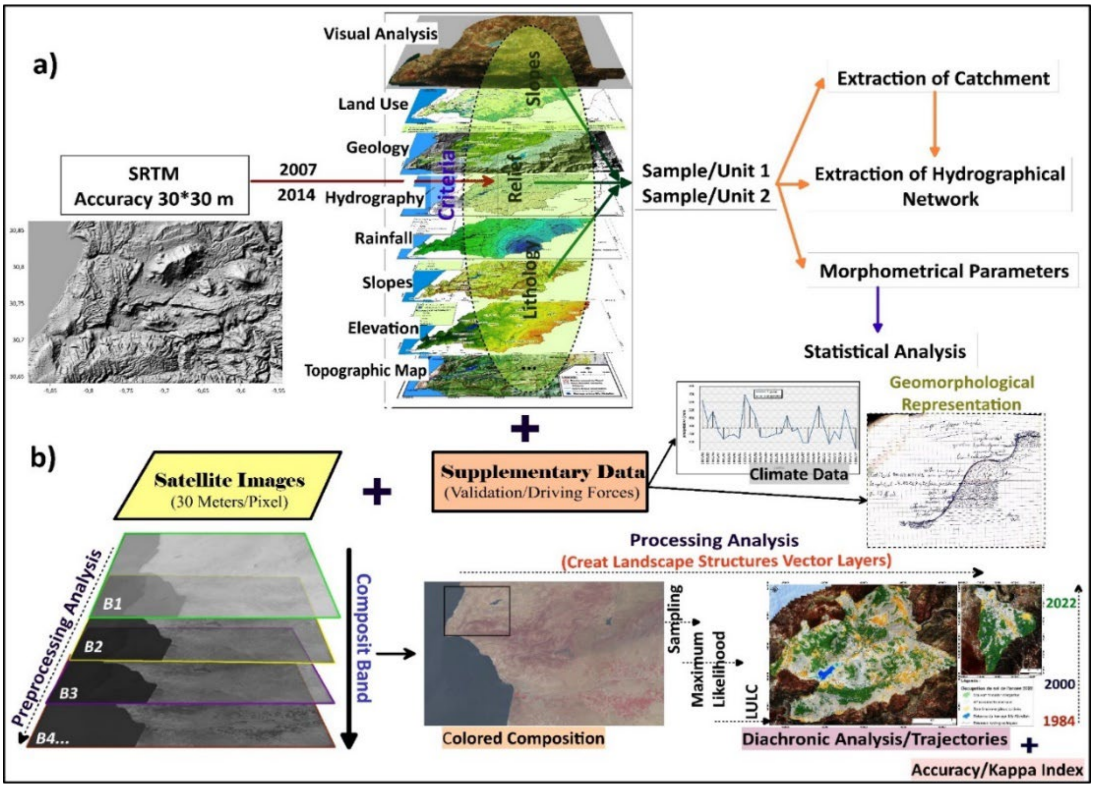

Figure 4. Methodological flowchart of the applied approaches: a) Methodology Adopted for the Identification of Sampling Units and Analysis of DEMs, b) Remote sensing analysis and supplementary data used to validation.

Monthly and annual precipitation datasets were obtained from the Climate NASA Power website data series. To ensure coherence with land use/land cover dynamics, we limited the analysis to 1981 to 2022. To calculate the drought index for the study area, we applied and calculated the standardized precipitation index (SPI), and spatialized it over each 41-year periods between 1981-2022 based on statistical analysis, in order to examine the change in rainfall rates and the recurrence of drought years. The Standardized Precipitation Index (SPI), developed by (McKee *et al.*, 1993), is used to pinpoint wet and dry periods based on long-term precipitation records. As detailed in Table 2, drought intensity correlates directly with SPI values. Specifically, negative anomalies, beginning at -2, signal drought conditions. These periods are considered to end when SPI values transition to positive, signifying wet conditions at +2. We use the following formula (1) (Schneider *et al.*, 2013):

$$SPI = (P-P^*) / \sigma_p \quad (1)$$

where P = precipitation, p* = mean precipitation, and, σp = standard deviation of precipitation.

Table 2. SPI values (McKee et al.*, 1993)*

SPI value	Class
2.0+	Extremely wet
1.5 to 1.99	Very wet
1.0 to 1.49	Moderately wet
-0.99 to 0.99	Near normal
-1.0 to -1.49	Moderately dry
-1.5 to -1.99	Severely dry
-2 and less	Extremely dry

3.2. Morphometric ratios and indexes

The study used a dataset derived from Digital Elevation Models (DEMs) to quantify and assess the evolution of gullies and marly slopes (Jafari *et al.*, 2024). This involved calculating various indices and ratios (related to area, length, relief, etc.) for different stream orders, which were then comparatively analyzed between the Aziar and Ighzer Ougadir units for 2007 and 2014. The difference between the 2007 and 2014 values was used to model disturbances in landscape functioning caused by natural and human factors. Additionally, the hypsometric curve and integral were calculated to detail the geomorphological and topographical characteristics of the two units.

- **Hypsometric analysis**: The topography created by stream-channel erosion, along with weathering, mass movement, and sheet runoff, is highly complex. This complexity is evident in both the intricate shapes of the landforms and the interrelated processes that shape them (Strahler, 1952b). The shape of the hypsometric curve and the integral value indicates notable differences among regions at various stages of development and geological structures. In less degraded landscapes, the hypsometric integral is high, but decreases as the landscape undergoes erosion and approaches the mature and old age stages (Pareta and Pareta, 2012; Strahler, 1952a, 1952b). Based on DEM data, we construct the hypsometric curves (Schumm, 1956; Strahler, 1952a) and calculate the indexes and ratios shown in (Table 3 and 4).

Table 3. Shape and relief parameters.

Index	Formula	Parameters	Source
Gravelius Index	*Kg=P/2*√∏*A*	P: perimeter of the BV/ ∏=3.14 and A: Surface area of the watershed	(Karalis *et al.*, 2014; Schumm, 1956)
Equivalent rectangle	*L=Kg√A/1.12*(1+√1-(1.12/Kg)²)*	L: Length, Kg : Gravelius index	(Horton, 1945)
Basin relief (Bh)	*Bh = h – h1*	h = maximum height (m) h1 = minimum height (m)	(Culler *et al.*, 1961)
Useful height difference	*Du= H5-H95*	H5: Z5% H95: Z95%	(Roche, 1963)
Theoretical Slope	$TS= B_h/L$	ΔH: variation of max and min heights/ L: Length of the watershed	(Roche, 1963)
Useful slope	*Ig= Du/L*	ΔH: variation of heights 5% and 95% / L: Length of the watershed	(Roche, 1963; Schumm, 1956)
Specific Height Difference	*Ds= Ig√A*	Us: Useful slope A: Area (km)	(Roche, 1963)
Dissection Index (Dis)	$Dis = B_h/Ra$	Bh= Bassin relief Ra= Absolute relief	(Singh and Dubey, 1994)
Elongation Ratio (Re)	$R=1,128\sqrt{A}/ L_{eb}$	A = area of the basin (km2) Lb = basin length	(Schumm, 1956)
Hypsometric Integral (HI)	*Hi= (Hm - h) / (H - h)*	Hm = the weighted mean elevation, H= maximum elevation, h= minimum elevation	(Duan *et al.*, 2022; Strahler, 1952a, 1957, 1964)

Table 4. Hydrographic parameters.

Index	Formula	Parameters	Source
Hydrographic Density	$Dh= \sum Ni/A$	Ni: the total stream numbers of all orders (km-²) A: is area of the watershed (km²)	(Horton, 1945)
Drainage Density	$Dd= Lu/A \sum Li$	Lu: the total stream length of all orders (km) A: is area of the watershed (km²)	(Horton, 1945)
Length Ratio	$R_L= Ln+1\ L_n$	Where, Ln+1 denotes the total length of watercourses of order n+1 (in km), while Ln is the total length of watercourses of order n (in km).	(Horton, 1945)
Confluence Ratio	$Rc= N_n / N_{+1}$	Where, N_n denotes the total number of watercourses of order in Nth order, and N_{+1} is the total number of stream in the next higher order	(Schumm, 1956)

- **The Dissection Index** (Di), as shown in Table 4, is a way to measure the amount of vertical erosion and the development stage of landforms in a watershed (Singh and Dubey, 1994). The scale ranges from 0.0, indicating an absence of dissection and dominance of flat terrain, to 1.0, which is observed in rare instances like vertical cliffs along coastlines or steep hill escarpments (Farhan *et al.*, 2015). The classification of watersheds according to their degree of dissection is as follows (Farhan *et al.*, 2015):
  - Flat-undulating (Di value < 0.1)
  - Rolling (0.1 - 0.4)
  - Moderately dissected (0.4 - 0.7)
  - Highly dissected (0.7 - 1.0)
  - Extremely dissected (>1.0)
- **Topographic Wetness Index** (TWI): is a crucial geomorphological tool that maps saturation zones, which are variable source areas for runoff. The TWI predicts the location of these saturated areas where the upslope contributing area is large and the local slope is small (i.e., in concave, converging areas of the landscape) (Hitouri *et al.*, 2024; Moore *et al.*, 1991). The TWI is defined as ln(a/tan β), where tan β represents the local slope of the ground surface (2). The 'a', as the specific upslope area, is calculated as the ratio of the upslope area (A in m²) to the contour length (L in m) (3) (Sørensen and Seibert, 2007). The topographic wetness index has been widely applied to characterize the influence of topography on the location and extent of saturated source areas responsible for runoff generation. Based on DEM treatment, the topographic wetness index is applied following a series of equation using Raster Calculator in ArcGIS software (2), (3), (4), (5) (Berhanu and Bisrat, 2018; Ruhoff *et al.*, 2011):

$$\text{Slope } \beta = ((\text{Slope map} * 1.570796))/90 \quad (2)$$

$$\text{Tan Slope } \beta = \text{Con (Slope >0, Tan Slope), 0.001)} \quad (3)$$

$$\text{FlowAccum-scaled= ((FlowAccum+1) * Cell size)} \quad (4)$$

$$\text{TWI} = ln\ (\text{FlowAccum} - \text{scaled})/\tan\ \beta \quad (5)$$

The Topographic Wetness Index (TWI) assigns higher values to areas with extended upslope regions (greater water retention) and lower values to smaller upslope regions (steeper, better-drained areas) (Sørensen and Seibert, 2007). The study area was categorized into five terrain classes using cluster analysis: wetland, humid topography, quite wetland, quite dry land, and dry land. The wetland and humid categories occupy low-lying, flood-prone areas, while dry land is concentrated at higher elevations.

- **Sediment Transport Index** (STI): The process of gully erosion indicate that the flow transports material from the disintegration of gully heads, floors, and sides, depositing it downstream when the flow diminishes (Garres-Díaz *et al.*, 2022). Modeling sediment transport provides valuable insights into the potential for sediment transport within a catchment's stream network. To calculate this index using ArcGIS, different input raster is required such as DEM of study area, Flow Direction Layer, Flow Accumulation Layer and Slope Layer (6). The Sediment Transport Index (STI) can be calculated as proposed by (Moore and Burch, 1986) using the Raster Calculator tool in ArcGIS, with the equation below.

$$STI= (m+1) * (As/22.13, 0.6)^{m} * Sin(\beta)/0.0896)^{n} \quad (6)$$

Where: As represents the specific catchment area (the area contributing upslope per unit contour length), estimated using one of the flow accumulation algorithms available in hydrology toolboxes; β is the local slope gradient in degrees; the contributing area exponent, m, typically ranges from 0.4 to 0.6; and the slope exponent, n, generally falls between 1.3 and 1.6 (Moore and Burch, 1986).

- **Stream Power Index (SDI):** is essentially a secondary topographic attribute derived directly from flow accumulation and slope, and it quantifies the erosive power of flowing water. It shows that runoff has a high erosive power on convex slopes. However, flow accumulation tends to concentrate at the base of convex slopes and within concave slopes (Wilson and Lorang, 2000). It is determined by a combination of slope and upslope contributing area, making it useful for identifying areas susceptible to gully formation. The SDI for a given grid cell (i) is calculated using the following equation (Micu and Urdea, 2022; Wilson and Lorang, 2000) (7):

$$SDIi = ln\,(DAi \times \tan(Gi)) \quad (7)$$

Where, SDI is the stream power index, DAi, is the product of the flow accumulation at a grid cell and the grid cell area, and Gi is the slope at a grid cell.

3.3. Field-work study and approach

In this study, we adopted a systemic and multidisciplinary approach to investigate the factors affecting the dynamics of marly slope landscapes in the lower valley of Wadi Tamri. To carry out the landscape surveys of toposequences, we applied a practical methodology, starting by designing a sampling grid of the landscape structure. Thirty-eight (38) sites were selected based on the variety of slope conditions (Irifi and Tribak, 2024b) (Fig. 5). Fieldwork for this study was carried out on March 10, 2021, December 23, 2020, March 25, 2021, January 16 and 19, 2022, and February 2, 2022, across the two marly slope landscape structures. Additionally, the inventory was essentially conducted during the rainy season. In the fieldwork, sampling was conducted, focusing on surveying erosional forms and processes and providing a general description of various ecological, morphological and anthropic variables. In each plot, identified by x and y coordinates through the *MAPinr* application, data on erosion forms and their evolutionary processes across the three slope sections were recorded (Irifi, 2023; Irifi and Tribak, 2024b).

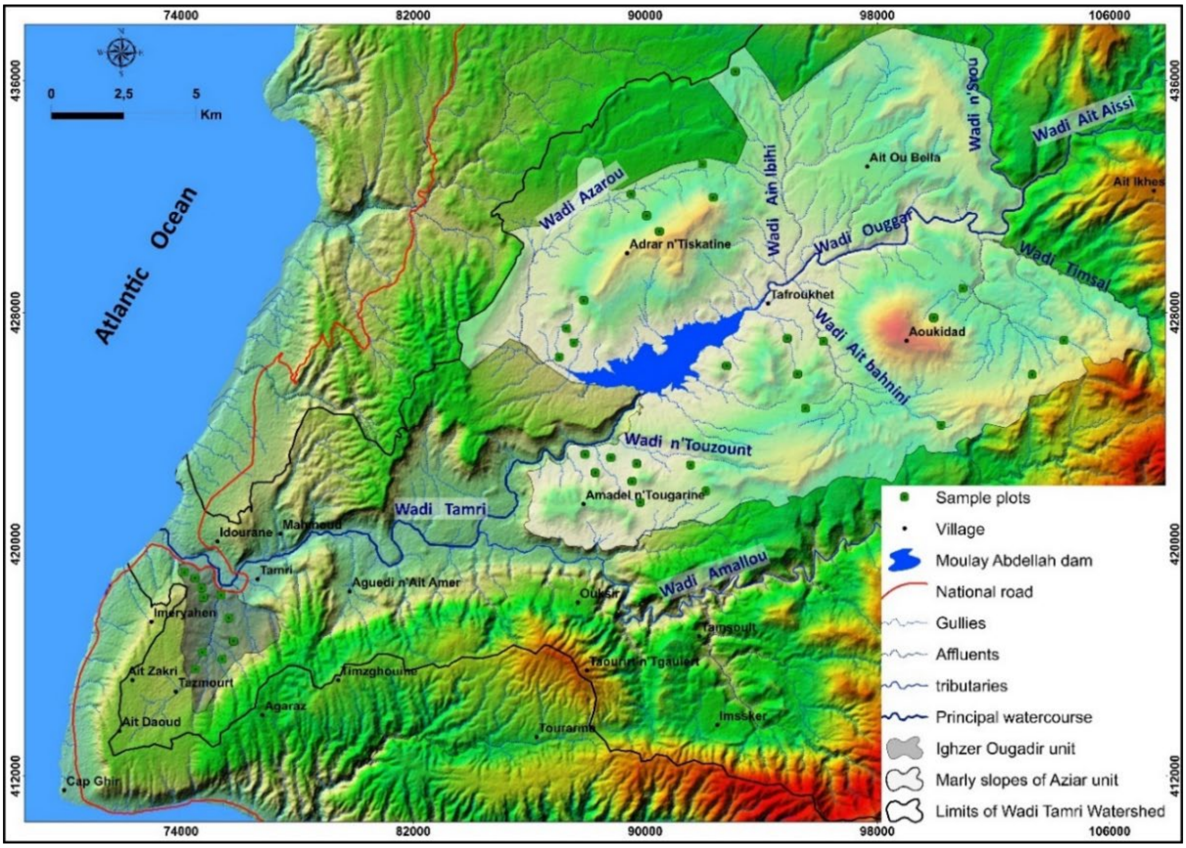

Figure 5. Location of the sampling plots.

The primary goal of the field inventory and sampling method was to establish toposequences and analyze the causal link between biotic and abiotic factors influencing the landscape. The inventory recorded variables for each slope section, including: field conditions (elevation, slope, bedrock, soil, exposure), ecological factors (tree cover type/density, regeneration, shrub recovery rate), and erosion features/processes (soil conditions, surface formations, and human activities impacting the factors). The ultimate aim was to investigate the correlation between natural factors (lithology, soil type, slope, exposure, vegetation) and human activities. The fieldwork in the evaluated plots was conducted using: the satellite imagery obtained from the *SAS.planete* image sensor (Irifi and Tribak, 2024a), the identification of plant species at each assessed sample point, based reference materials such as the book by (Benabid, 2000), and the scientific paper by (Irifi and Tribak, 2021), along with the "PlantNet" smartphone application (Asshoumy and Rahayu, 2023; Wäldchen and Mäder, 2018). We are considering the type, distribution, sociability and root systems of species capable of developing and protecting such a hostile marl substratum.

4. Results

4.1. Geomorphometric Analysis

The hypsometric curve reveals the volume of rock mass in a watershed and the degree of erosion that has taken place relative to the remaining mass. Consequently, the hypsometric integral serves as an indicator to assess the erosion status of the watershed (Bishop, 2002; Farhan *et al.*, 2015; Joseph Markose *et al.*, 2014). The hypsometric curve of the two units, especially for the Ighzer Ougadir unit, exhibits an S-shaped pattern, with a hypsometric integral of 0.49 and 0.5. indicating that the landscape is transitioning from the youth to the mature stage of geomorphic evolution, reflecting a terrain that has experienced extended erosion during the quaternary, leading to an airier landscape. In the two units, Di values range from 0.82 to 0.87, indicating a highly dissected landscape shaped by multiple phases of erosion and neotectonic activity (Table 5). When (Re) values are low, as seen with 0.6 for the Ighzer Ougadir basin and 0.41 for the Aziar watershed, it indicates that the watersheds are elongated and possess high relief and steep slopes. The Specific Height Difference values (130.7 m and 159.2 m) also highlight the relatively steep terrain (Table 5).

The Ighzer Ougadir unit, classified into six stream orders, exhibits an extremely high hydrographic density (543 km^{-2} in 2007 and increasing to 598.59 km^{-2} in 2014). This high density is attributed to the impermeable rocks, low vegetation cover, and steep terrain. The analysis showed a 5% increase in gullying between 2007 and 2014. In 2014, the unit contained 5,537 total gullies spanning 368.81 km. The first-order streams were the most dominant, with 3,245 gullies (totaling 261.25 km) but having the shortest average length (0.08 km per gully). Overall, the data confirms a correlative evolution across the watershed orders, with hydrographic density decreasing from order 1 to order 6 (Fig. 6). The comparative study of the drainage network between 2007 and 2014 revealed an overall increase in drainage density in both the Ighzer Ougadir and Aziar landscape units, signaling heightened erosion likely due to vegetation loss. Specifically, the Aziar unit saw the number of first-order gullies surge from 69,253 to 77,999. While the total and average lengths of these gullies slightly decreased, the minimal changes observed in the bifurcation (2.19 to 2.20) and length ratios for higher orders (3, 5, 6) suggest that the network's efficiency in sediment transport remained relatively stable despite the increased extension of the drainage system (Fig. 7).

Table 5. Shape and relief parameters.

Index	Ighzer Ougadir unit	Aziar unit
Gravelius Index	1.35 (Semi elongated basin)	1.75 (elongated basin)
Equivalent rectangle	5.97 km	42.17 km
Basin relief (Bh)	361 m	855 m
Useful height difference	245 m	440 m
Theoretical Slope	60.4 m/km	20.3 m/km
Useful slope	41 m/km (Very high slopes)	10.4 m/km (very high slopes)
Specific Height Difference	130.7 m (relatively steep terrain)	159.2 m (relatively steep terrain)
Dissection Index (Di)	0.87 (highly dissected relief)	0.82 (highly dissected relief)
Elongation Ratio (Re)	0.60 (elongated shape and high relief and steep slopes)	0.41 (elongated shape and high relief and steep slopes)
Hypsometric Integral (HI)	0.49	0.5

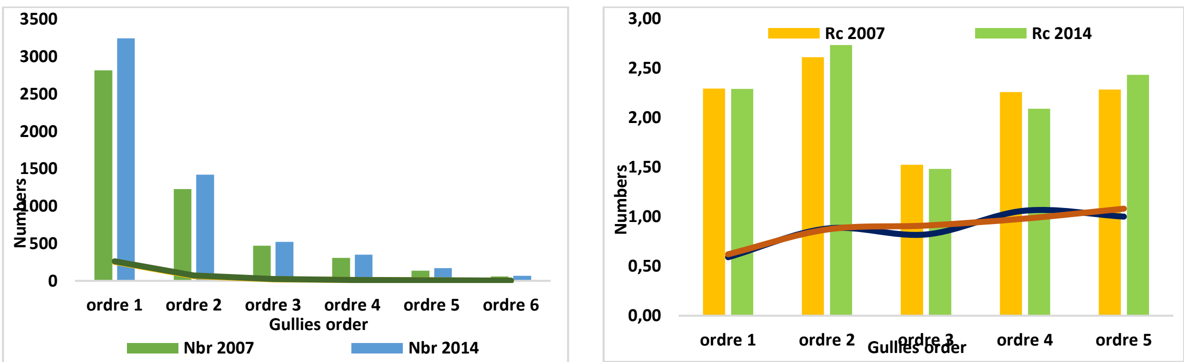

RC: Confluence Ratio and RL: Length Ratio.

Figure 6. Characteristics of hydrographic parameters in the Ighzer Ougadir sub-catchment. Source: DEM https://search.asf.alaska.edu/ and https://earthexplorer.usgs.gov 2007/2014.

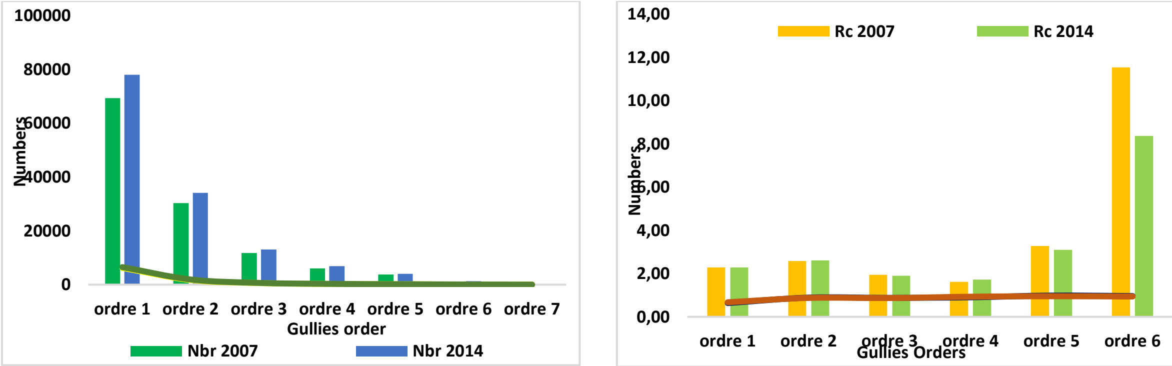

RC: Confluence Ratio and RL: Length Ratio.

Figure 7. Characteristics of hydrographic parameters in the Aziar landscape unit. Source: DEM https://search.asf.alaska.edu/ and https://earthexplorer.usgs.gov 2007/2014.

To enhance this analysis, we compute the topographic index, which describes the spatial distribution of soil moisture, water depth, surface saturation and associated landscape processes (Berhanu and Bisrat, 2018; Leh and Chaubey, 2009; Meles *et al.*, 2020; Qin *et al.*, 2011). The integrated analysis of the Topographic Wetness Index and the Sediment Transport Index reveals a landscape dominated by dry soil conditions and high erosive potential. TWI analysis (2007 and 2014) consistently showed a widespread lack of moisture accumulation, with 'very dry' cells constituting ≈40% of the area, even within hydric soil zones. Wetter conditions are confined mainly to the main watercourse and the Moulay Abdellah Dam (low-slope areas). The corresponding STI analysis successfully mapped the spatial distribution of erosion, indicating that the highest erosive potential (STI ≥170) is concentrated along the hydrographic network (orders 4-7) and ravines. This directly demonstrates the significant role of topography in localizing and driving soil erosion and sediment transport (Fig. 8).

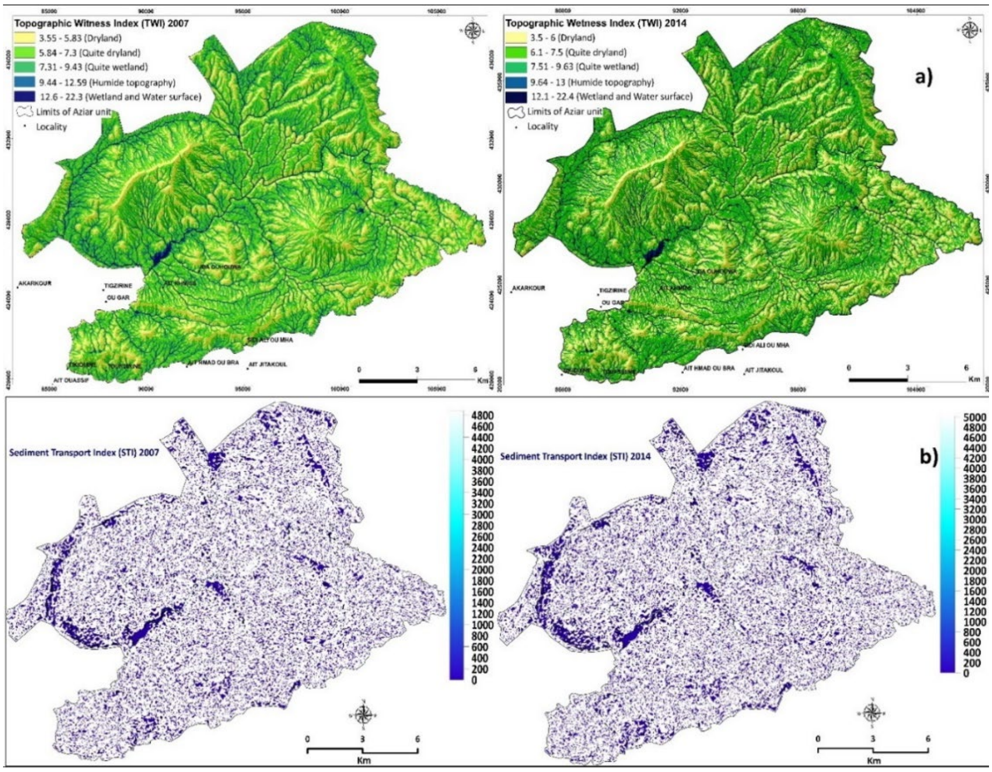

Figure 8. a) Topographic Wetness Index, and b) Sediment Transport Index of Aziar landscape unit in 2007 (left) and 2024 (right). Source: DEMs https://search.asf.alaska.edu/#/?dataset=ALOS

The Stream Power Index (SPI) analysis from 2007 to 2014 revealed a significant increase in the erosive activity of gullies on the marl slopes, a dynamic reflected by a shift toward positive SPI values (indicating a strong capacity to erode and evacuate sediment). The maps, showing SPI values mostly between -6 and 5.5, highlight those areas initially stable or characterized by sedimentation (values ≤0) became susceptible to gully erosion, particularly on steep slopes. This widespread erosion is likely driven by the strong decrease in protective forest cover combined with rainfall variability over the period. Low SPI values (between -6 and -0.5) remain characteristic of gentle, stable areas like riverbeds and vegetated zones (Fig. 9).

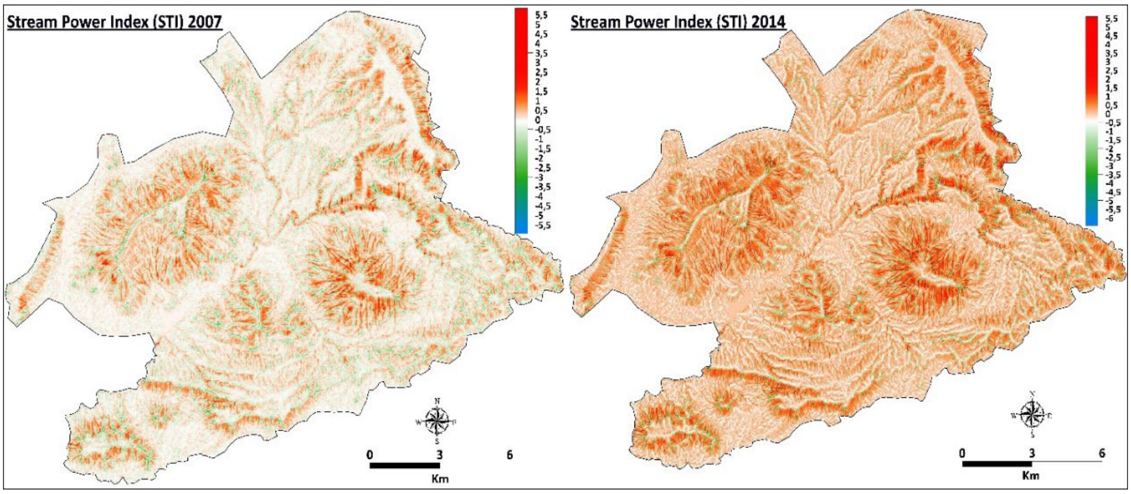

Figure 9. Stream Power Index of Aziar landscape unit in 2007 (left) and 2024 (right). Source: DEMs https://search.asf.alaska.edu/#/?dataset=ALOS

4.2. Land use change and dry years recurrence as a driving force of slopes dynamics

The research utilized a diachronic analysis of biotic, abiotic, and anthropogenic factors, along with a 1981-2022 rainfall analysis, to understand gully dynamics. Results confirm a clear trend toward slope instability, marked by forest landscape regression and increased human encroachment. Between 1984 and 2000, both the Ighzer Ougadir and Aziar units showed land cover degradation: Ighzer Ougadir experienced a slight vegetation decrease and increased marly substratum, while Aziar saw a significant loss of vegetation concurrent with a large increase in agricultural land (from 1,957 ha to 3,941 ha). However, the trend in the Aziar unit reversed between 2000 and 2022, showing a positive shift toward argan forest recovery (≈219 ha increased) and a decrease in cultivated land, suggesting more sustainable practices. Despite this positive trend, the marl substratum continues to extend, indicating the complex, ongoing influence of human activities and deforestation on land cover change (Table 6 and Fig. 10) (Tribak, 1998).

The period between 1984 and 2022 saw a clear landscape transformation characterized by the significant regression of Argan forest cover (-26%) in favor of marly rocks (+5%) and cultivated soils. This decline is attributed to the conversion of vegetated areas into agricultural fields (crops, terraces, grazing) and other anthropogenic pressures like mechanized Argan undergrowth cultivation, charcoal production, and fossil extraction (Table 7). The rate of degradation is highly dependent on geology: Hauterivian green marls are the most susceptible, suffering from dominant gullying leading to complete denudation, while Aptian formations show high stability and dense forest cover. Albian blue marls exhibit moderate erosion with branching gully networks due to their gypsiferous content. Overall, the data confirms a degrading biotic component linked to socio-spatial changes and erosive geomorphological activity.

Table 6. Evolution of land uses and changes in the marl landscape units (ha).

Land use (Ighzer Ougadir unit)	1984	2000	2022	1984-2000	2000-2022	1984-2022
Forest class of Argan tree	445.76	433.34	463.00	-12.42	29.66	17.24
Marly substratum	414.71	434.10	347.00	19.39	-87.10	-67.71
Cultivated silty-clay	60.08	50.78	111.00	-9.30	60.22	50.92
Land use (Aziar unit)	**1984**	**2000**	**2022**	**1984-2000**	**2000-2022**	**1984-2022**
Forest class of Argan tree	9281.57	6625.12	6844.51	-2656.45	219.39	-2437.06
Marly substratum	12045.30	11788	12679.30	-257.30	891.30	634
Cultivated silty-clay	1957.10	3941.76	3596.21	1984.66	-345.55	1639.11

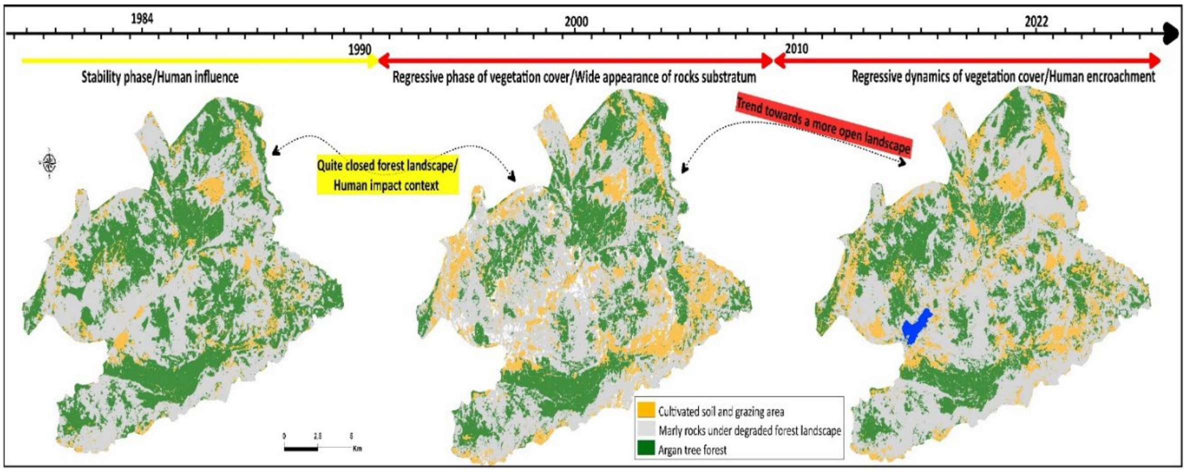

Figure 10. Different landscape trajectories in the Aziar units.

Table 7. Rate of change in land use classes in the marl landscape units (%).

Class of Ighzer Ougadir unit	Evolution rate 1984-2000	Evolution rate 2000-2022	Evolution rate 1984-2022
Forest class of Argan tree	-3%	7%	4%
Marly substratum	5%	-20%	-16%
Cultivated silty-clay	-15%	119%	85%
Class of Aziar unit	**Evolution rate 1984-2000**	**Evolution rate 2000-2022**	**Evolution rate 1984-2022**
Forest class of Argan tree	-29%	3%	-26%
Marly substratum	-2%	8%	5%
Cultivated silty-clay	101%	-9%	84%

The primary challenge facing the landscape is the striking erosion and denudation of agricultural and forest land, particularly evident at the foot of mountains like Amadel Tiskatine and Jbel Aoulkjdade. This erosion is dominated by gullying, characterized by the lateral widening and regressive retreat of gully heads, which is progressively creating a badlands landscape. Gullying affects a substantial 7% of the total area (over 1,668 ha), while 13% remains stable (2,929 ha). However, the most concerning statistic is that the majority of marl slopes are highly susceptible to gullying, accounting for 65% (over 15,115 ha) of the total landscape unit area (Irifi, 2023). The risk of gullying is not limited to natural slopes but also severely impacts terraced farmland, leading to its destruction, often due to abandonment or poor maintenance. Crucially, most slopes exposed to gullying are categorized as silvipastoral land, likely former cleared areas that are now bare and highly susceptible to intense erosion.

Landsat satellite imagery confirms a significant loss of vegetation cover and a corresponding expansion of the marly substratum across both study areas. This regressive landscape change is primarily driven by rainfall variability, increased dry years, and major shifts in traditional land use, all contributing to higher erosion susceptibility on the marly slopes. The study's land use classification proved highly accurate, achieving a 92% overall accuracy and a robust Kappa coefficient of 0.89, validating the reliability of the satellite image analysis (Table 8) (Foody, 2020; Rwanga and Ndambuki, 2017). Therefore, our calculated Kappa coefficient of 0.89 indicates a very good or significantly high rate.

Data from the Tamri climate stations (1981–2022) reveal a significant downward trend in total rainfall in the Atlantic High Atlas since the early 2000s, consistently staying below the 260 mm average. The period was characterized by high annual variability, including three short wet periods and six prolonged dry spells, with the years 1999–2009 being particularly severe. This reduced precipitation has severely compromised the natural regeneration and sustainability of the forest landscape, directly causing a marked decline in vegetation cover and the widespread abandonment of agricultural land between 2000 and 2022 (Fig. 11) (Irifi and Tribak, 2024a).

According to the classification developed by (McKee *et al.*, 1993), the study area experienced short periods of near-normal drought (indices ranging from -0.99 to 0.99), as well as a dominant drought scenario ranging from moderately dry to extremely dry (indices ranging from -0.99 to -2). The analysis of the 12-month Standardized Precipitation Index (SPI) confirms the region, particularly the Tamri and Agadir stations, is experiencing severe drought conditions, unlike neighboring areas. Data from 1981 to 2022 shows the Tamri station has been predominantly in drought, frequently registering SPI anomalies below -2. While short wet periods occurred, the frequency and intensity of prolonged droughts have notably increased since 2000, significantly impacting the local forests and agriculture (Fig. 12).

Table 8. Classification Accuracy Assessment and Confusion matrix of Landsat 8 OLI (09/2022).

	Forest class of Argan tree	***Marly substratum***	***Cultivated silty-clay***	***Water***	***U-Total***	***U-Accuracy***	***Kappa***
Forest class of Argan tree	25	0	0	0	25	1	
Marly substratum	2	19	0	0	21	0,90	
Cultivated silty-clay	1	2	12	0	15	0,80	
Water	0	0	0	5	5	1	
P-Total	28	21	12	5	66		
P-Accuracy	0,89	0,90	1	1		0,92	
***Kappa* Coefficient**							**0,89**

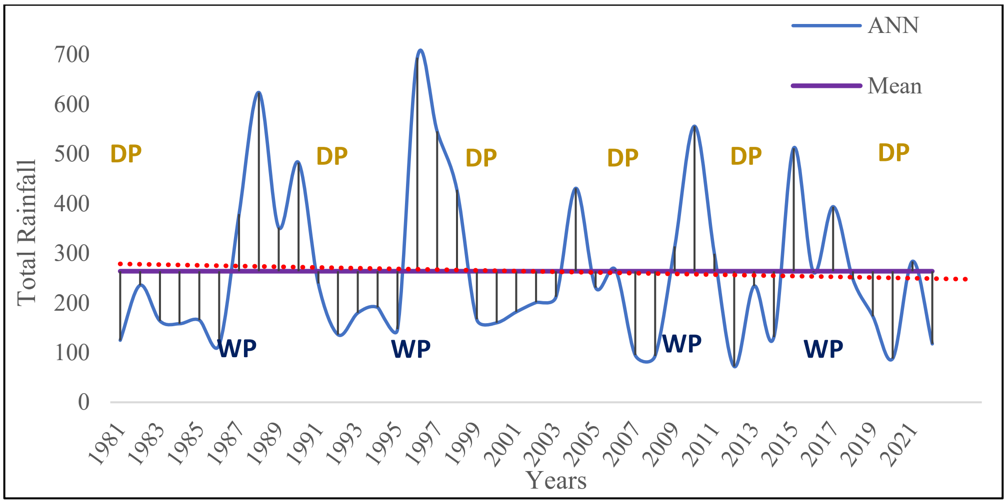

Figure 11. Rainfall Variability in the Tamri station between 1981 to 2022. WP: Wet Period, DP: Dry Period. Source https://power.larc.nasa.gov/data-access-viewer

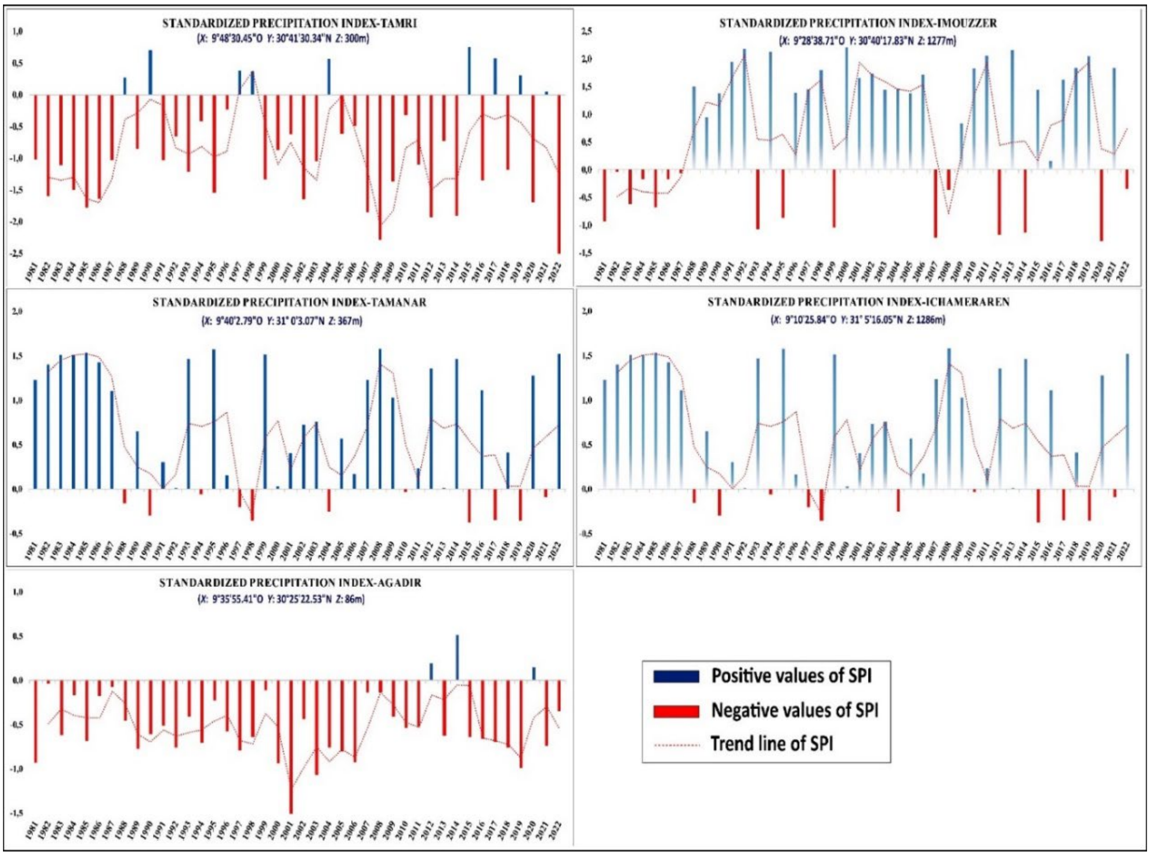

Figure. 12. SPI Temporal Variation (12-Month Scale) in the Atlantic High Atlas (1981-2022). Source https://power.larc.nasa.gov/data-access-viewer

4.3. Toposequences and gullies characteristics

The marly slopes of the lower Wadi Tamri valley are severely impacted by heavy erosion and gullying, leading to the formation of badlands (Irifi and Tribak, 2024b). These erosional landforms are primarily developed on Hauterivian lithological formations (marl, clay, lumachellic limestone), which are relatively soft. The intensity and variety of erosion are driven by a combination of factors, including lithological contrasts, tectonics, climate, low vegetation cover, and human activities (García-Ruiz *et al.*, 2013; Moreno-de Las Heras and Gallart, 2018). Due to minimal vegetation and active cultivation, the marls are easily displaced as mudflows, followed by linear erosion (Tribak, 1998). A close look at the slope profiles confirms this, revealing landscapes that are typically bare, stripped, and ruiniform (Fig. 13 and 14).

The landscape of the study area, particularly the Ighzer Ougadir unit, is a highly diverse and zoned environment fundamentally shaped by mid-Cretaceous marly formations and Plio-Quaternary tectonics (Weisrock, 1980). This geological control, coupled with climate and human activities, dictates erosion and land use patterns (Farhan *et al.*, 2015; Hunt *et al.*, 2023). The slopes exhibit clear vertical zonation, upper Slopes are capped by resistant Moghrebian cliffs (Weisrock, 2012; Weisrock *et al.*, 2017), mid-slopes are Highly prone to erosion, featuring shallow soils over marly and colluvial deposits. Lower slopes show better stabilization due to forest vegetation and feature deep, well-drained sandy-loam soils often organized into stepped terraces. However, the prevalence of underlying marl, especially where cultivated, makes vast areas susceptible to extensive gullying and piping erosion (Bovi *et al.*, 2020), particularly the less-stabilized sandy-silty low terraces (Irifi and Tribak, 2024b) (Fig. 13).

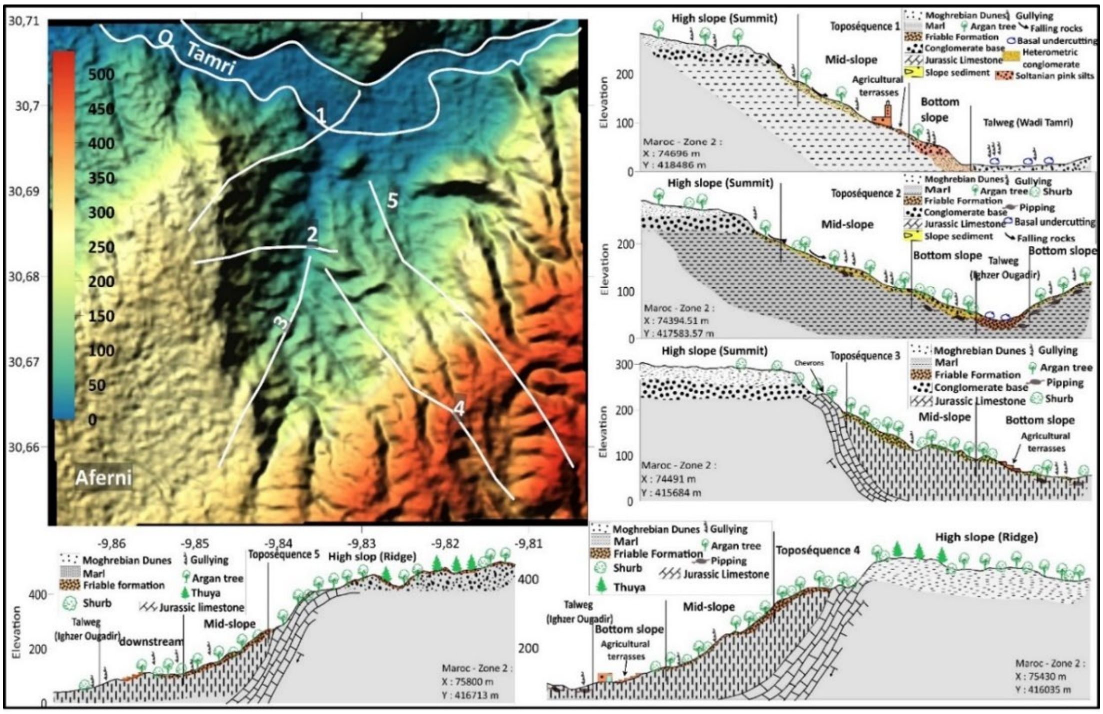

Figure 13. Toposequences of the Ighzer Ougadir unit.

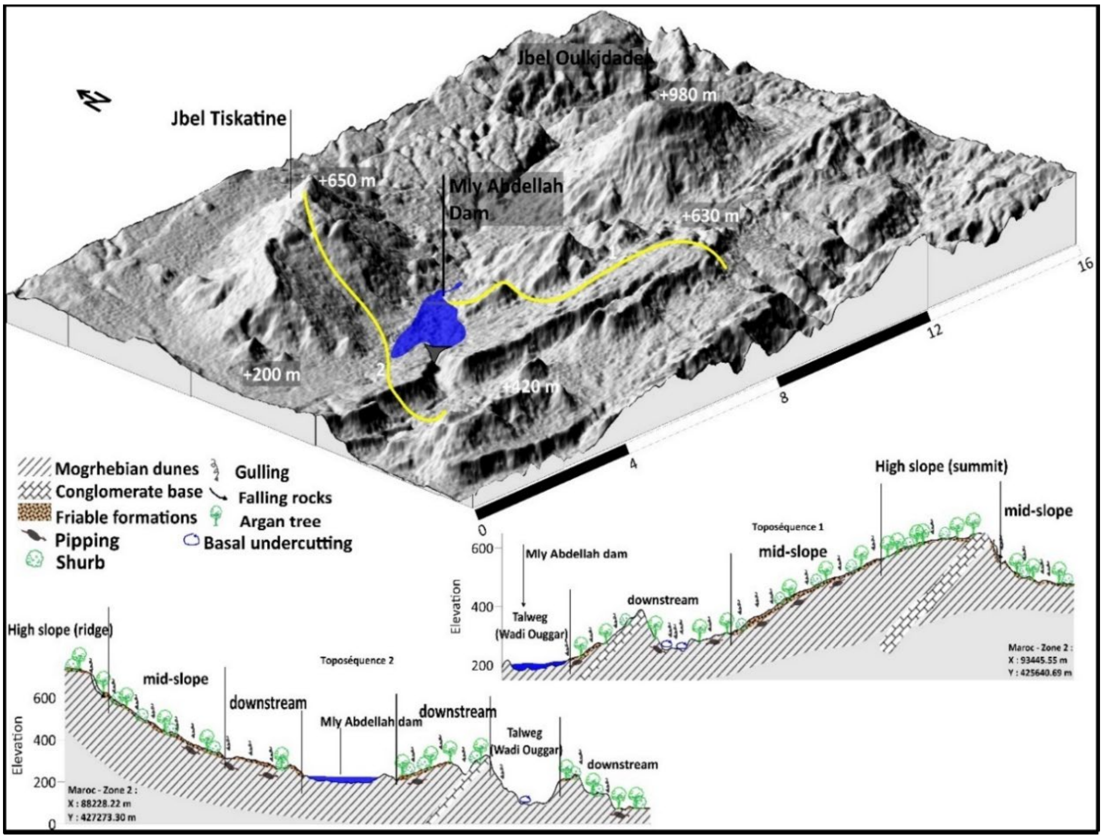

Figure 14. Toposequences of the Aziar unit.

The Aziar landscape unit exhibits a clear erosional zonation driven by geology and slope. The high-slope section, facing south, is composed of limestone and marls covered by thin soils, where karstic processes and boulder falls are common due to the underlying, lacerated green marl destabilizing the limestone above. This area supports only sparse, degraded argan vegetation. The mid-slope is defined by friable formations and steepness, making it highly susceptible to intense linear erosion, ranging from initial gullying to badlands formation, often intensified by piping processes (Irifi and Tribak, 2024a). Conversely, the lower slopes feature colluvial brown deposits reshaped into stepped terraces (El Ouahidi, 2008; Irifi, 2023; Irifi and Tribak, 2021). Even here, the exposed marl substratum is subject to constant erosion, including scratches, gullies, and active piping (Tribak, 1998, 2020; Tribak *et al.*, 2021), despite supporting species like *Argania spinosa* and *Launea arborescens* (Fig. 14).

Erosion across the marl slopes is highly variable, dictated by slope angle, aspect, geotechnical conditions, and human activity (El Khalili *et al.*, 2013; Faulkner, 2018; García-Ruiz *et al.*, 2013; Maquaire *et al.*, 2003; Moreno-de Las Heras and Gallart, 2018). The most significant erosion form is gullying, characterized by V-shaped, hierarchical gullies that converge into deep ravines. These gully walls show signs of small scars and detachments, even on gentler slopes (Maquaire *et al.*, 2003; Tribak, 1998; Vandekerckhove *et al.*, 2000; Xu *et al.*, 2019). Field surveys identified five main categories of land instabilities associated with degraded forest cover: areolar erosion, linear erosion, gravity movements, karstic erosion, and fluvial dynamics, affecting the totality of the lower valley. Marls are less permeable formations with poor cohesion, rendering them highly susceptible to solifluction and gully formation. In the Aziar landscape unit, gullying is intensified by differential erosion between hard limestone banks and soft marl layers, coupled with the regressive erosion actively occurring at the gully heads and walls (Fig. 15).

Figure 15. Forms of erosion affecting marl slopes in the lower Oued Tamri valley (Author: Irifi, H. 2020-2022). a) Appearance of Badlands landforms, on Marls, b) Regressive duck-step erosion, c) Developing gully, d) landscape of Badlands, e) Slaking crust, f) Basal scarping of the Ighzer Ougadir fluvial formations combined with piping, g) Fall of large boulders detached from the Moghrebian dead cliff, h) Piping and terrace scree.

5. Discussion

The quantitative study of the marl slopes in the lower Wadi Tamri valley analyzed 19 morphometric and hydrological parameters (including drainage, sediment transport, and topographic humidity) to assess the hydrographic network's characteristics and dynamics. The results confirm that the drainage patterns reflect the friability of the marly lithology under semi-arid conditions and the ongoing vegetation degradation. High drainage and hydrographic density values emphasize the bedrock's impermeability and the streams' substantial capacity for sediment evacuation (Evans, 2012; Farhan *et al.*, 2015; Migoń and Latocha, 2018). Overall, the morphometric ratios highlight the area's severe susceptibility to gullying and slope remodeling, with the Stream Power Index identifying bare soil with steep slopes as the zone most prone to ravine development and sediment transport. The morphometric analysis highlights the significant development and active erosional processes within the drainage network, indicated by a high Dissection Index (Di ≈0.87 to 0.82). The bifurcation rate, which influences the sediment concentration time, is crucial; a lower rate allows for faster sediment evacuation (Benzougagh *et al.*, 2019; Farhan *et al.*, 2015; Strahler, 1957, 1964). The evolution between 2007 and 2014 saw major changes, including the branching and bifurcation of medium-order networks, shifts in stream order, and stream capture (diversion of flow). These dynamics underscore the landscape transformation and the ongoing struggle between erosion and sedimentation in the study area (Fig. 16 and 17).

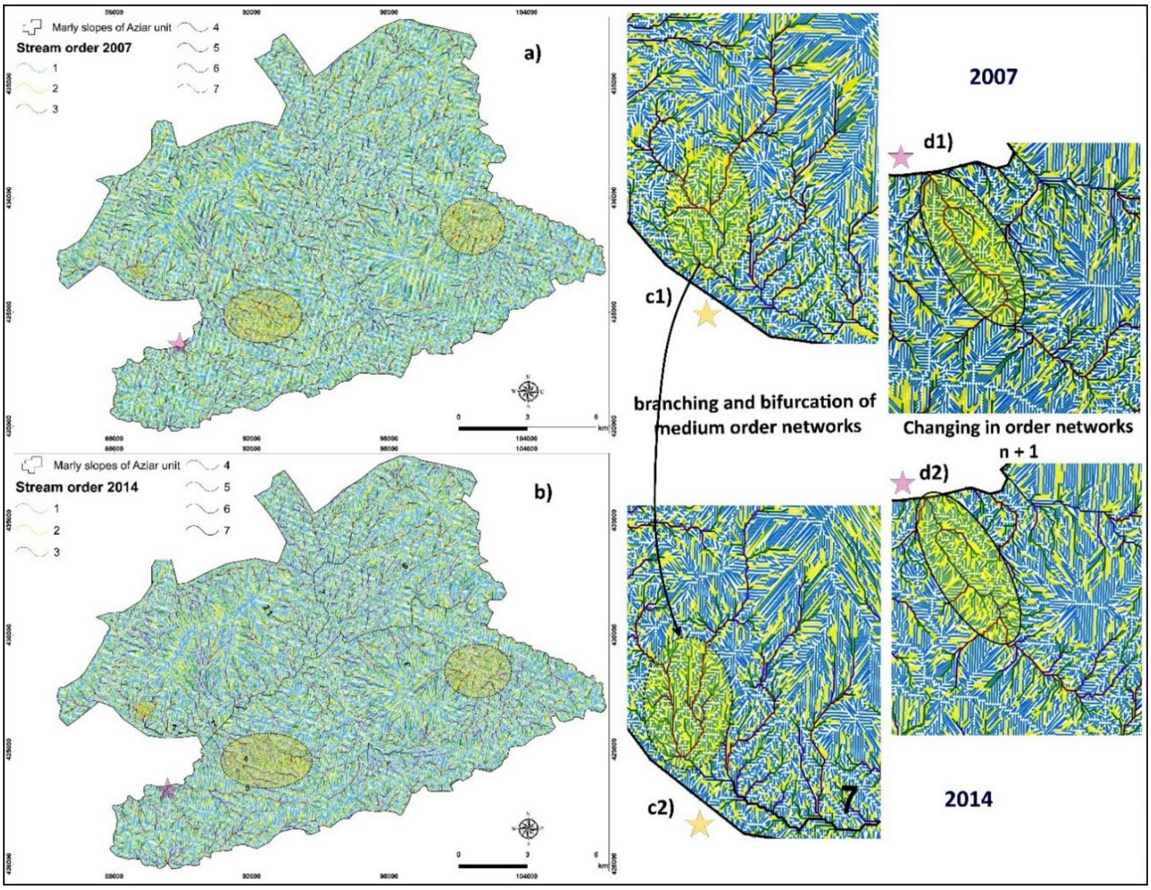

Figure 16. Example of stream network development between 2007 and 2014 in the Aziar landscape units. a) Hydrographic network in 2007, b) hydrographic network in 2014, c1) example of hydrographic network change in 2007, c2) hydrographic network change in 2014, d1) Example of hydrographic network change in 2007, d2) Hydrographic network change in 2014. Source: DEMs https://search.asf.alaska.edu/#/?dataset=ALOS

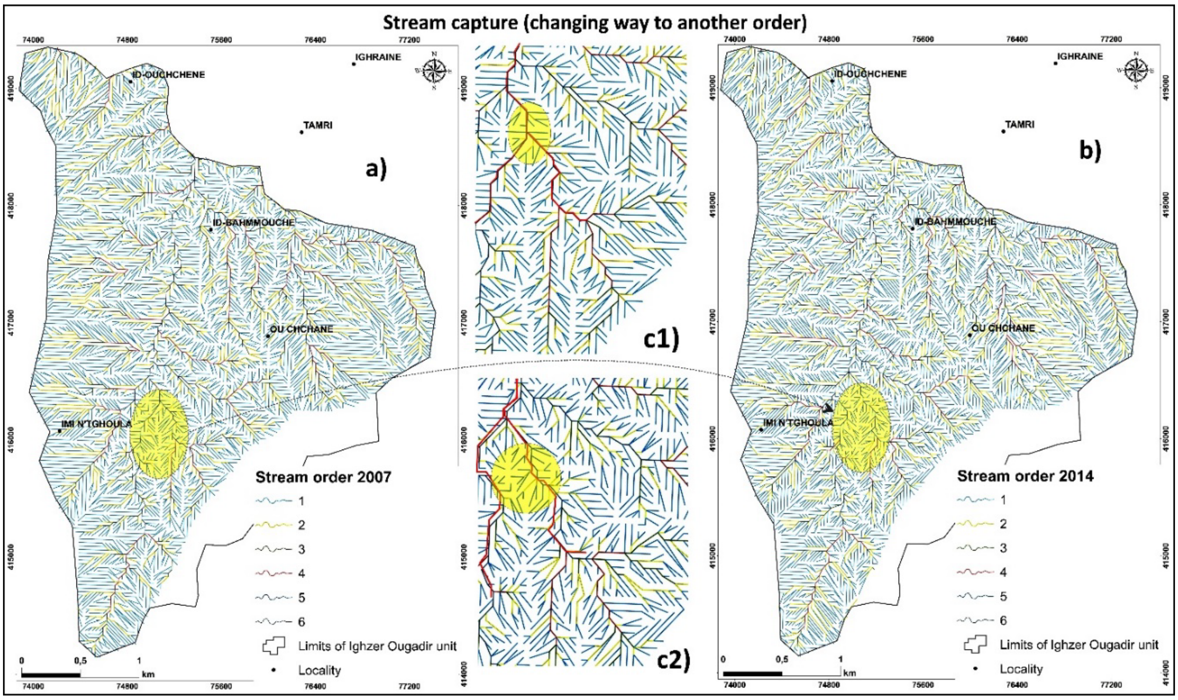

Figure 17. Example of stream network development between 2007 and 2014 in the Ighzer Ougadir units: a) Hydrographic network in 2007, b) hydrographic network in 2014, c1) example of hydrographic network change in 2007, c2) hydrographic network change in 2014. Source: DEMs https://search.asf.alaska.edu/#/?dataset=ALOS

Erosion studies conducted by (Tribak, 1998) on the Miocene marls of the Tarmast region in eastern Prerif confirm that the rapid development of gullies and significant sediment production are driven by a six-part interaction of processes on marl formations. Key mechanisms include the gravitational fall of material (due to desiccation and cracking in dry periods), intense gully wall erosion by scratch networks (accelerated during rain), and frequent localized landslides during wet seasons caused by basal undermining and water saturation (Tribak, 1998). Additionally, piping, or subsurface erosion, contributes, often facilitated by salts. Furthermore, research on network expansion suggests that the drainage network's shape is determined by the external flow field, not internal stream flow, and that emerging groundwater can initiate and advance channel heads (Devauchelle *et al.*, 2012; Petroff *et al.*, 2013).

The diachronic analysis of gully dynamics reveals intense and accelerated gully formation in both landscape units between 2007 and 2014, evident in the increased number and length of gullies. The rising Length Ratio for stream order 1 specifically confirms the dominance of headcut and regressive erosion in driving gully evolution and bifurcation, primarily affecting the first- and second-order gullies (Farhan *et al.*, 2015; Grecu *et al.*, 2007; Karalis *et al.*, 2014; Panda *et al.*, 2019). The variation in gully activity between the Ighzer Ougadir and Aziar units is strongly correlated with differences in lithology, vegetation cover, and the presence of anti-erosion features (terraces, gabions) (Bannari *et al.*, 2017). Furthermore, the TWI and STI indices strongly correlate with the observed erosion patterns, showing that while dry slopes prevail, the expansion of wet topography within the stream network (per the 2014 DEM) suggests heightened susceptibility to gully erosion, confirming that sediment consistently flows from elevated terrain to susceptible downstream areas (Hitouri *et al.*, 2024).

The quantitative and qualitative geomorphometric analysis of the Wadi Tamri study area is validated by findings from the Wadi Kerak in Jordan, which shares similar climatic challenges like slope instability, soil erosion, and deforestation (Farhan *et al.*, 2015). In both regions, relief and shape parameters confirm the high susceptibility to gully erosion and active geomorphological evolution. Specifically, the Wadi Kerak analysis showed a highly dissected landscape with high bifurcation ratios (indicating strong structural control) and a high relief ratio (pointing to active erosion and steep slopes). This makes the basin highly prone to landslides, soil erosion, and high surface runoff (Farhan *et al.*, 2015). Similarly, the Wadi Tamri and the Wadi Inaouène watershed in Morocco both show pronounced erosion vulnerability driven by the combination of steep slopes, limited plant cover, and widespread marl substratum, which together intensify surface runoff and promote gully proliferation (Benzougagh *et al.*, 2019; Srinivasa Vittala *et al.*, 2004).

In the Algerian Sebkhas region, research has emphasized the erosion of aeolian deposits, whose unconsolidated nature make them far more susceptible to incision than the surrounding lithified outcrops or compacted clays. This high erodibility drives rapid gully development, ultimately carving the landscape into high-density drainage networks characteristic of badland topography (Bousba *et al.*, 2024). The landscape evolution from to shows a transition from a relatively dense forest to a phase of environmental instability, driven by the interaction of natural and man-made processes at the interface of different geological formations. This 38-year period is marked by the significant regression of argan tree cover, which has been replaced by expanding marly rock and cultivated or grazed soils. Agricultural encroachment and recurrent droughts are the primary factors leading to the decline in forest cover and the increase in bare marl substratum and low-fertility land (Goudie, 2023). This deterioration signals a profound imbalance in the local agro-sylvopastoral system, heavily reliant on the now-diminishing tree cover (Irifi, 2023; Irifi and Tribak, 2024a). Our analysis revealed the following:

(i) The area covered by argan forests and their associated flora has gradually declined over time;

(ii) forest cover has noticeably densified, transitioning from medium to low (sparse) density;

(iii) a general regression trend is apparent, though it exhibits spatial and temporal disparities depending on the area and period.

The fragile landscapes of the study area are suffering from severe agroforestry pressures dating back to the French Protectorate. Conflicts arising from state land appropriation led to locals illegally cutting or burning trees to reduce landscape density, creating friction with the Water and Forestry Administration. This, combined with unauthorized and managed tree felling (often for free fodder), has led to severely imbalanced forest ecosystems on the Aziar plateaux. Compounded by semi-arid, drought-ridden conditions and intense pastoral strain, these areas face ongoing biodiversity loss, diminished natural regeneration, and the creation of landforms highly susceptible to erosion, ensuring the continued decline of vegetation cover (Irifi and Tribak, 2024a).

The forest landscapes of the lower Wadi Tamri valley are rapidly deteriorating due to a semi-arid climate and intense human pressure, resulting in increasing erosion rates (Irifi and Tribak, 2024a). With only one exception (Ain Tamaloukt forest), the remaining forest massifs (Ait Khemiss, Aoujdad, etc.) urgently require management plans to ensure their conservation. The documented geomorphological degradation and complex landscape situation necessitate developing a comprehensive landscape action plan to integrate all concerns, facilitate effective collaboration among partners, and address the pressing issues of degradation and instability (Irifi *et al.*, 2020).

The core finding is the need for an integrated landscape approach to develop and enhance the mountainous Wadi Tamri region, moving past current isolated, sector-based management. This approach aims to promote concerted action among all stakeholders to conserve forestry and edaphic resources. By recognizing the landscape's heterogeneity and integrating the needs of the local population, a comprehensive local development project can be designed, addressing wide-ranging challenges, including agroforestry, tourism, heritage preservation, and soil erosion control. The central challenge is the rehabilitation and restoration of forest resources, requiring the establishment of defenses and the enhancement of pastoral potential by restoring palatable species. Given the observed decline in forest resources and silvopastoral activity, their conservation is urgent. The recommended solution is a concerted and participatory management approach, involving close collaboration among agriculture, water, and forest administrations and the local population. This collaborative approach transforms the landscape resource into a powerful tool for local development and effectively identifies the region's vulnerabilities (Peyrache-Gadeau and Perron, 2020).

To protect the landscape and control soil degradation, crucial actions are needed to minimize the silting-up of dams (like the Prince Moulay Abdellah dam). This involves immediately implementing mechanical and biological correction techniques-such as sills, gabions, low stone walls, and reforestation-to counter severe erosive activity in large and medium-sized ravines. Prioritization should be given to areas behind the Prince Moulay Abdellah dam reservoir, the Aguedi n'Ait Amer depression, and the southern Haha plateaus, along with large-scale reforestation around dam perimeters to protect the banks (Fig. 18). To enhance landscape integrity and sustainability, the study recommends developing tourism activities for sustainable engagement and establishing a legal framework to regulate the currently indiscriminate extraction of Mesozoic fossils (ammonites, echinoderms, etc.). Furthermore, it proposes increasing floristic and faunistic biodiversity through the reintegration of various species, while promoting ancestral conservative water and soil management techniques, such as slope terracing and the Iferd technic (Irifi, 2023).

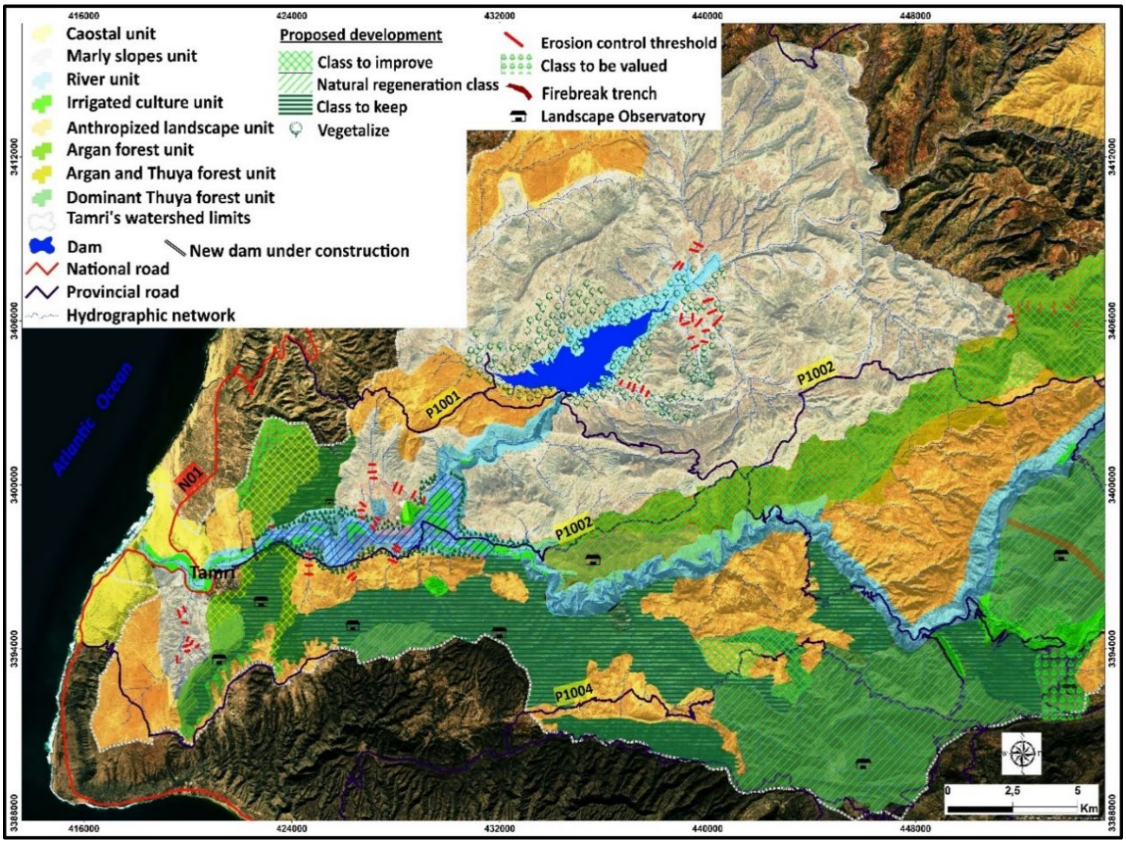

Figure 18. Proposed valorization actions on the landscape units' map.

6. Conclusion

A comprehensive, integrated analysis of the lower Wadi Tamri marly slopes, utilizing geomorphometric analysis, remote sensing (GIS), and toposequences studies, has provided crucial insight into the landscape's dynamics. This approach unveiled substantial landscape alterations over recent decades, driven primarily by significant drought recurrence, widespread degradation, and the proliferation/elongation of gully networks. The interplay of these factors has led to significant changes in the region's topography and ecological balance, with distinct patterns of gully development identified through comparison between 2007 and 2014. The study confirms the drainage network has undergone significant alterations, including increased stream order, branching, and stream capture, driven by an accelerated gullying process and sediment production on marly slopes. Regressive erosion (gully head and bank retreat) is dominant in areas with homogeneous lithology, while differential erosion combines with regressive processes in heterogeneous zones. Over seven years, steep and medium slopes showed a significant increase in the number and length of gullies. High values from the Sediment Transport Index (STI), Topographic Wetness Index (TWI), and Stream Power Index (SPI) confirm high erosion potential and sediment transport capacity, particularly concentrated along the hydrographic network and ravines of lower-order streams (1, 2, 3, and 4). Gully development and accelerated erosion on the marl slopes near the Moulay Abdellah dam are driven by a complex interaction of climatic aggressiveness, slope inclination, land use changes, and soil properties, seriously threatening the dam's storage capacity. The study focused on two units, finding that the proliferation of gullies, intensified by subsurface flow, leads to various erosion patterns, including linear erosion, solifluction, and landslides. Crucially, the erosion and gullying, which affect 65% of the slopes, are severely exacerbated by human activities such as stripping bare agricultural and forest lands and the destruction of terraced farmland through abandonment. This human-induced pressure accelerates lateral spreading and headcutting, transforming vulnerable slopes into extensive badlands. Despite limitations (lack of geotechnical and precise sedimentation rate analysis), the integrated remote sensing, geomorphometric, and fieldwork data provide a scientific basis for planning a communal gully control project. The findings of this study underscore the vulnerability of marly slopes, especially those surrounding the Moulay Abdellah Dam. The application of this integrated methodology within a systemic analysis identifies key drivers of land degradation-specifically gully evolution, soil properties, vegetation regression, and unsustainable human practices- which must be managed to protect this fragile Mediterranean environment.

Acknowledgments

Deep thanks and gratitude to the Editor of the journal and all anonymous reviewers for suggestions and comments.

Author contribution and conflicts of interest

IH assumed the tasks of data collection through field work and the use of documents (maps, archive documents, satellite images, numerical data, statistical bases, etc.). He also ensured the development of the databases and the various figures as well as the interpretation and verification of the results in the field. TA provided direction and supervision of the work, analysis and interpretation of data, correction of the manuscript, validation of the results as well as the development of language.

The authors undertake to disclose any existing or potential conflict of interest in relation to the publication of this article.

References

Adams, A.E. (1979). Sedimentary environments and palaeogeography of the western High Atlas, Morocco, during the Middle and late jurassic. *Palaeogeography, Palaeoclimatology, Palaeoecology 28*, 185-196. https://doi.org/10.1016/0031-0182(79)90118-4

Alves, G.B., Oliveira, F.S.D., Silva, A.H.N.D., Souza, V S.D. (2024). Toposequence: What are we talking about? *Revista Brasileira de Ciência Do Solo 48*, e0230137. https://doi.org/10.36783/18069657rbcs20230137

Ambroggi, R. (1963). *Etude géologique du versant méridional du Haut Atlas occidental et de la plaine du Souss* [Thèse de doctorat, Université de Paris]. Notes et Mémoires du Service Géologique (Rabat). http://pascal-francis.inist.fr/vibad/index.php?action=getRecordDetail&idt=19271626

Amhani, Z., Tribak, A. (2022). Cartographie de l'utilisation des sols et de l'érosion hydrique dans le bassin versant de l'Oued Lahdar (Prérif oriental-Maroc) : Utilisation des données de la télédétection et du modèle RUSLE. *Bollettino dell'Associazione Italiana di Cartografia* 171, 4-20. https://doi.org/10.13137/2282-572X/33429

Aouragh, M.H., Ijlil, S., Essahlaoui, N., Essahlaoui, A., El Hmaidi, A., El Ouali, A., Mridekh, A. (2023). Remote sensing and GIS-based machine learning models for spatial gully erosion prediction: A case study of Rdat watershed in Sebou basin, Morocco. *Remote Sensing Applications: Society and Environment 30*, 100939. https://doi.org/10.1016/j.rsase.2023.100939

Asshoumy, S.Z., Rahayu, E.S. (2023). The Effect of Analyzing Images Using the PlantNet Application and TGT on Motivation, Classification Abilities, and Data Presentation in Plantae Material. *Journal of Biology Education 12*(3), 314-322.

Bammou, Y., Benzougagh, B., Abdessalam, O., Brahim, I., Kader, S., Spalevic, V., Sestras, P., Ercişli, S. (2024). Machine learning models for gully erosion susceptibility assessment in the Tensift catchment, Haouz Plain, Morocco for sustainable development. *Journal of African Earth Sciences 213*, 105229. https://doi.org/10.1016/j.jafrearsci.2024.105229

Bannari, A., Ghadeer, A., El-Battay, A., Hameed, N.A., Rouai, M. (2017). Detection of Areas Associated with Flash Floods and Erosion Caused by Rainfall Storm Using Topographic Attributes, Hydrologic Indices, and GIS. In S. Pirasteh and J. Li (Éds.), *Global Changes and Natural Disaster Management: Geo-information Technologies* (pp. 155-174). Springer. https://doi.org/10.1007/978-3-319-51844-2_13

Benabid, A.A. (2000). *Flore et écosystèmes du Maroc : Évaluation et préservation de la biodiversité.* Ibis Press, Paris; Librairie et Éditions Kalila Wa Dimna, Rabat.

Benzougagh, B., Dridri, A., Boudad, L., Sdkaoui, D., Baamar, B. (2019). Apport des Sig et Teledetection pour L'evaluation des Caracteristiques Physiques du Bassin Versant d'oued Inaouene (Nord-Est Maroc) et leurs Utilites dans le Domaine de la Gestion des Risques Naturels. *American Journal of Innovative Research and Applied Sciences 8*(4), 120-130.

Berhanu, B., Bisrat, E. (2018). Identification of Surface Water Storing Sites Using Topographic Wetness Index (TWI) and Normalized Difference Vegetation Index (NDVI). *Journal of Natural Resources and Development 8*, 91-100. https://doi.org/10.5027/jnrd.v8i0.09

Bishop, M. (2002). Geomorphic change in high mountains: A western Himalayan perspective. *Global and Planetary Change 32*(4), 311-329. https://doi.org/10.1016/S0921-8181(02)00073-5

Bousba, H., Marmi, R., Chabour, N., La Licata, M., De Amicis, M., Bosino, A. (2024). Assessment of geomorphological landforms and features in the Sebkhas region of the Boulhilet Plain, north-eastern Algeria. *Geografia Fisica e Dinamica Quaternaria 47*(2), 349-364. https://doi.org/10.4454/85jg6bn4

Bovi, R.C., Moreira, C.A., Rosolen, V.S., Rosa, F.T.G., Furlan, L.M., Helene, L.P.I. (2020). Piping process: Genesis and network characterization through a pedological and geophysical approach. *Geoderma 361*, 114101. https://doi.org/10.1016/j.geoderma.2019.114101

Castillo, C., Taguas, E.V., Zarco-Tejada, P., James, M.R., Gómez, J.A. (2014). The normalized topographic method: An automated procedure for gully mapping using GIS. *Earth Surface Processes and Landforms 39*(15), 2002-2015. https://doi.org/10.1002/esp.3595

Catani, F., Segoni, S., Falorni, G. (2010). An empirical geomorphology-based approach to the spatial prediction of soil thickness at catchment scale. *Water Resources Research 46*(5), 2008WR007450. https://doi.org/10.1029/2008WR007450

Charton, R., Kluge, C., Fernández-Blanco, D., Duval-Arnould, A., Bryers, O., Redfern, J., Bertotti, G. (2021). Syn-depositional Mesozoic siliciclastic pathways on the Moroccan Atlantic margin linked to evaporite mobilisation. *Marine and Petroleum Geology 128*, 105018. https://doi.org/10.1016/j.marpetgeo.2021.105018

Chen, Q., Mudd, S.M., Attal, M., Hancock, S. (2024). Extracting an accurate river network : Stream burning re-revisited. *Remote Sensing of Environment 312*, 114333. https://doi.org/10.1016/j.rse.2024.114333

Ciccolini, U., Bufalini, M., Materazzi, M., Dramis, F. (2024). Gully Erosion Development in Drainage Basins: A New Morphometric Approach. *Land 13*(6), 792. https://doi.org/10.3390/land13060792

Cui, T., He, Y., Wang, L., Luo, J., Xiao, T., Liu, H., Zhang, B., Deng, Q., Yang, H. (2024). Characteristics and development of steepland gullies in the dry valleys of Southwest China. *PeerJ 12*, e18411. https://doi.org/10.7717/peerj.18411

Culler, R.C., Hadley, R., Schumm, S.A. (1961). Hydrology of the upper Cheyenne River basin : Part A. Hydrology of stock-water reservoirs in upper Cheyenne River basin; Part B. Sediment sources and drainage-basin characteristics in upper Cheyenne River basin. *Water Supply Paper* 1531. https://doi.org/10.3133/wsp1531

Dai, W., Yang, X., Na, J., Li, J., Brus, D., Xiong, L., Tang, G., Huang, X. (2019). Effects of DEM resolution on the accuracy of gully maps in loess hilly areas. *Catena 177*, 114-125. https://doi.org/10.1016/j.catena.2019.02.010

Dai, W., Hu, G., Yang, X., Yang, X., Cheng, Y., Xiong, L., Strobl, J., Tang, G. (2020). Identifying ephemeral gullies from high-resolution images and DEMs using flow-directional detection. *Journal of Mountain Science 17*(12), 3024-3038. https://doi.org/10.1007/s11629-020-6084-5

Devauchelle, O., Petroff, A.P., Seybold, H.F., Rothman, D.H. (2012). Ramification of stream networks. *Proceedings of the National Academy of Sciences 109*(51), 20832-20836. https://doi.org/10.1073/pnas.1215218109

Dewitte, O., Daoudi, M., Bosco, C., Van Den Eeckhaut, M. (2015). Predicting the susceptibility to gully initiation in data-poor regions. *Geomorphology 228*, 101-115. https://doi.org/10.1016/j.geomorph.2014.08.010

Duan, Y., Pei, X., Zhang, X. (2022). The Hypsometric Integral Based on Digital Elevation Model for the Area West of Lvliang Mountains in Loess Plateau, Shanxi, China. *Frontiers in Earth Science 10*. https://doi.org/10.3389/feart.2022.827836

El Aroussi, O. (2013). Modelling and Mapping of Soil Erosion On the Oued El Malleh Catchment Using Remote Sensing and GIS. *Journal of Urban and Environmental Engineering 7*(2), 302-307. https://doi.org/10.4090/juee.2013.v7n2.302307

El Garouani, A., Chen, H., Lewis, L., Tribak, A., Abahrour, M. (2009). Cartographie de L'utilisation du Sol et de l'érosion Nette à partir d'images Satellitaires et du SIG IDRISI au Nord-Est du Maroc. *Revue Télédétection 8*(3), 193-201.

El Khalili, A., Raclot, D., Habaeib, H., Lamachère, J.M. (2013). Factors and processes of permanent gully evolution in a Mediterranean marly environment (Cape Bon, Tunisia). *Hydrological Sciences Journal 58*(7), 1519-1531. https://doi.org/10.1080/02626667.2013.824086

El Ouahidi, A. (2008). *Etude morphosédimentaire des héritages pléistocènes et holocènes de la basse vallée de l'oued Tamri (Maroc)* [Thèse de doctorat]. Université Nancy 2.

Emberger, L. (1925). Le domaine naturel de l'Arganier. *Bulletin de la Société Botanique de France 72*(4), 770-774. https://doi.org/10.1080/00378941.1925.10832788

Evans, I.S. (2012). Geomorphometry and landform mapping: What is a landform? *Geomorphology 137*(1), 94-106. https://doi.org/10.1016/j.geomorph.2010.09.029

Evans, M., Lindsay, J. (2010). High resolution quantification of gully erosion in upland peatlands at the landscape scale. *Earth Surface Processes and Landforms 35*(8), 876-886. https://doi.org/10.1002/esp.1918

Farhan, Y., Anbar, A., Enaba, O., Al-Shaikh, N. (2015). Quantitative Analysis of Geomorphometric Parameters of Wadi Kerak, Jordan, Using Remote Sensing and GIS. *Journal of Water Resource and Protection 07*(06), 456-475. https://doi.org/10.4236/jwarp.2015.76037

Faulkner, H. (2018). The Role of Piping in the Development of Badlands. In E. Nadal-Romero, J.F. Martínez-Murillo, N.J. Kuhn (eds.), *Badlands Dynamics in a Context of Global Change* (pp. 191-216). Elsevier. https://doi.org/10.1016/B978-0-12-813054-4.00006-X

Foody, G.M. (2020). Explaining the unsuitability of the kappa coefficient in the assessment and comparison of the accuracy of thematic maps obtained by image classification. *Remote sensing of environment 239*, 111630.

García-Ruiz, J.M., Nadal-Romero, E., Lana-Renault, N., Beguería, S. (2013). Erosion in Mediterranean landscapes: Changes and future challenges. *Geomorphology 198*, 20-36. https://doi.org/10.1016/j.geomorph.2013.05.023

Garres-Díaz, J., Fernández-Nieto, E.D., Narbona-Reina, G. (2022). A semi-implicit approach for sediment transport models with gravitational effects. *Applied Mathematics and Computation 421*, 126938. https://doi.org/10.1016/j.amc.2022.126938

Goudie, A. (2023). Water Erosion and Mass Movements. In A. Goudie, *Landscapes of the Anthropocene with Google Earth* (pp. 191-219). Springer Nature Switzerland. https://doi.org/10.1007/978-3-031-45385-4_9

Grecu, F., Zăvoianu, I., Zaharia, L., Comănescu, L. (2007). Analyse quantitative du réseau hydrographique du bassin versant du Slănic (Roumanie). *Physio-Géo*, *Volume 1*, 79-93. https://doi.org/10.4000/physio-geo.1051

Hayakawa, Y.S., Oguchi, T. (2006). DEM-based identification of fluvial knickzones and its application to Japanese mountain rivers. *Geomorphology 78*(1-2), 90-106. https://doi.org/10.1016/j.geomorph.2006.01.018

Hitouri, S., Meriame, M., Sk Ajim, A., Renata Pacheco, Q., Nguyen-Huy, T., Quoc Bao, P., ElKhrachy, I., Varasano, A. (2024). Gully erosion mapping susceptibility in a Mediterranean environment: A hybrid decision-making model. *International Soil and Water Conservation Research 12*(2), 279-297. https://doi.org/10.1016/j.iswcr.2023.09.008

Horton, R.E. (1945). Erosional Development of Streams and Their Drainage Basins; Hydrophysical Approach to Quantitative Morphology. *GSA Bulletin 56*(3), 275-370. https://doi.org/10.1130/0016-7606(1945)56[275:EDOSAT]2.0.CO;2

Hunt, A.G., Ghanbarian, B., Faybishenko, B. (2023). A model of temporal and spatial river network evolution with climatic inputs. *Frontiers in Water 5*, 1174570. https://doi.org/10.3389/frwa.2023.1174570

Irifi, H. (2023). *Dynamique des paysages de montagne : Paramètres, Impacts et Valorisation. Cas de la basse vallée de l'oued Tamri (Atlas Atlantique-Maroc).* [Thèse de doctorat]. Université Sidi Mohamed Ben Abdellah.

Irifi, H., Abdellatif, T., Ahmed, A. (2020). Paysages naturels dans la basse vallée de l'oued Tamri (Maroc) : Proposition de l'approche paysagère pour une valorisation touristique. *Geography Notebooks 3*(1), 1. https://doi.org/10.7358/gn-2020-001-irif

Irifi, H., Tribak, A. (2021). Diversité Floristique et Paysagère du Cours d'eau de la basse Vallée de l'oued Tamri (Haut Atlas Atlantique, Maroc). *Geomaghreb 17*, Article 17. https://revues.imist.ma/index.php/Geomaghreb/article/view/36972

Irifi, H., Tribak, A. (2024a). *Argania spinosa* and Tetraclinis articulata seedling regeneration factors in the lower valley of Wadi Tamri (Morocco). *Revista de Estudios Andaluces 48*, 133-150. https://doi.org/10.12795/rea.2024.i48.07

Irifi, H., Tribak, A. (2024b). Dynamique des Paysages Géomorphologiques des Versants Marneux et Sous Couvert Forestier dans La Basse Vallée de l'oued Tamri (Haut Atlas Atlantique -Maroc). In *Acte de congrès international sur les risques-Oujda*, pp. 160-166.

Jafari, M., Dehkordi, A.T., Kariminejad, N., Valadan Zoej, M.J., Shahabi, E., Quesada-Román, A. (2024). Comprehensive introduction to Digital Elevation Models, as a key dataset in soil erosion mapping. In *Advanced Tools for Studying Soil Erosion Processes* (p. 31-58). Elsevier. https://doi.org/10.1016/B978-0-443-22262-7.00023-0

Joseph Markose, V., Dinesh, A. C., Jayappa, K.S. (2014). Quantitative analysis of morphometric parameters of Kali River basin, southern India, using bearing azimuth and drainage (bAd) calculator and GIS. *Environmental Earth Sciences 72*(8), 2887-2903. https://doi.org/10.1007/s12665-014-3193-x

Karalis, S., Karymbalis, E., Valkanou, K., Chalkias, C., Katsafados, P., Kalogeropoulos, K., Batzakis, V., Bofilios, A. (2014). Assessment of the Relationships among Catchments' Morphometric Parameters and Hydrologic Indices. *International Journal of Geosciences 05*(13), 1571-1583. https://doi.org/10.4236/ijg.2014.513128

Leh, M.D., Chaubey, I. (2009). GIS-Based Predictive Models of Hillslope Runoff Generation Processes. *JAWRA Journal of the American Water Resources Association 45*(4), 844-856. https://doi.org/10.1111/j.1752-1688.2009.00328.x

Liu, B., Chen, Z., Li, B., Wu, S., Feng, H., Gao, X., Siddique, K.H.M. (2024). Modeling of driving factors and headcut rates of ephemeral gullies in the loess plateau of China using high-resolution remote sensing images. *International Journal of Digital Earth 17*(1), 2369632. https://doi.org/10.1080/17538947.2024.2369632

Maquaire, O., Malet, J.-P., Remaître, A., Locat, J., Klotz, S., Guillon, J. (2003). Instability conditions of marly hillslopes: Towards landsliding or gullying? The case of the Barcelonnette Basin, South East France. *Engineering Geology 70*(1-2), 109-130. https://doi.org/10.1016/S0013-7952(03)00086-3

McKee, T.B., Doesken, N.J., Kleist, J. (1993). *The Relationship of Drought Frequency and Duration to Time Scale*. In Proceedings of the 8th Conference on Applied Climatology (Vol. 17, pp. 179-183). American Meteorological Society.

Meles, M.B., Younger, S.E., Jackson, C.R., Du, E., Drover, D. (2020). Wetness index based on landscape position and topography (WILT) : Modifying TWI to reflect landscape position. *Journal of Environmental Management 255*, 109863. https://doi.org/10.1016/j.jenvman.2019.109863

Meliho, M., Khattabi, A., Mhammdi, N. (2018). A GIS-based approach for gully erosion susceptibility modelling using bivariate statistics methods in the Ourika watershed, Morocco. *Environmental Earth Sciences 77*(18), 655. https://doi.org/10.1007/s12665-018-7844-1

Micu, D., Urdea, P. (2022). Vulnerable Areas, the Stream Power Index and the Soil Characteristics on the Southern Slope of the Lipovei Hills. *Carpathian Journal of Earth and Environmental Sciences 17*(2), 207-218. https://doi.org/10.26471/cjees/2022/017/215

Migoń, P., Latocha, A. (2018). Human impact and geomorphic change through time in the Sudetes, Central Europe. *Quaternary International 470*, 194-206. https://doi.org/10.1016/j.quaint.2018.01.038

Moore, I.D., Burch, G.J. (1986). Sediment Transport Capacity of Sheet and Rill Flow: Application of Unit Stream Power Theory. *Water Resources Research 22*(8), 1350-1360. https://doi.org/10.1029/WR022i008p01350

Moore, I.D., Grayson, R.B., Ladson, A.R. (1991). Digital terrain modelling: A review of hydrological, geomorphological, and biological applications. *Hydrological Processes 5*(1), 3-30. https://doi.org/10.1002/hyp.3360050103

Moreno-de Las Heras, M., Gallart, F. (2018). The Origin of Badlands. Editors of the book In *Badlands Dynamics in a Context of Global Change* (p. 27-59). Elsevier. https://doi.org/10.1016/B978-0-12-813054-4.00002-2

Panda, B., Venkatesh, M., Kumar, B., Anshumali. (2019). A GIS-based Approach in Drainage and Morphometric Analysis of Ken River Basin and Sub-basins, Central India. *Journal of the Geological Society of India 93*(1), 75-84. https://doi.org/10.1007/s12594-019-1125-9

Pareta, K., Pareta, U. (2012). *Quantitative Geomorphological Analysis of a Watershed of Ravi River Basin, H.P. India*. https://www.semanticscholar.org/paper/Quantitative-Geomorphological-Analysis-of-a-of-Ravi-Pareta-Pareta/6cab7c899679b088433e5f789fa3222b7c376207

Paulinus, U.U., Ifedilichukwu, N.G., Ahamefula, A.C., Iheanyichukwu, O.A., Theophilus, E.T., Godwin Edet, I. (2016). Morphometric Analysis of Sub- watersheds in Oguta and Environs, Southeastern Nigeria Using GIS and Remote Sensing Data. *Journal of Geosciences and Geomatics 4*(2), 21-28. https://doi.org/10.12691/jgg-4-2-1

Peel, M.C., Finlayson, B.L., McMahon, T.A. (2007). Updated world map of the Köppen-Geiger climate classification. *Hydrology and Earth System Sciences 11*(5), 1633-1644. https://doi.org/10.5194/hess-11-1633-2007

Peter, K.D., d'Oleire-Oltmanns, S., Ries, J.B., Marzolff, I., Ait Hssaine, A. (2014). Soil erosion in gully catchments affected by land-levelling measures in the Souss Basin, Morocco, analysed by rainfall simulation and UAV remote sensing data. *Catena 113*, 24-40. https://doi.org/10.1016/j.catena.2013.09.004

Petroff, A.P., Devauchelle, O., Seybold, H., Rothman, D.H. (2013). Bifurcation dynamics of natural drainage networks. *Philosophical Transactions of the Royal Society A: Mathematical, Physical and Engineering Sciences 371*(2004), 20120365. https://doi.org/10.1098/rsta.2012.0365

Peyrache-Gadeau, V., Perron, L. (2020). Le Paysage comme ressource dans les projets de développement territorial. *Développement durable et territoires. Économie, géographie, politique, droit, sociologie 11*(2). https://journals.openedition.org/developpementdurable/17463

Qin, C.-Z., Zhu, A.-X., Pei, T., Li, B.-L., Scholten, T., Behrens, T., Zhou, C.-H. (2011). An approach to computing topographic wetness index based on maximum downslope gradient. *Precision Agriculture 12*(1), 32-43. https://doi.org/10.1007/s11119-009-9152-y

Roche, M. (1963). Hydrologie de surface. *Office De La Recherche Scientifique Et Technique Outre-Mer (ORSTOM) 1097*, 431.

Ruhoff, A.L., Castro, N.M.R., Risso, A. (2011). Numerical Modelling of the Topographic Wetness Index: An Analysis at Different Scales. *International Journal of Geosciences 02*(04), 476-483. https://doi.org/10.4236/ijg.2011.24050

Rwanga, S.S., Ndambuki, J.M. (2017). Accuracy assessment of land use/land cover classification using remote sensing and GIS. *International Journal of Geosciences 8*(04), 611.

Schneider, D. P., Deser, C., Fasullo, J., Trenberth, K. E. (2013). Climate Data Guide Spurs Discovery and Understanding. *Eos, Transactions American Geophysical Union 94*(13), 121-122. https://doi.org/10.1002/2013EO130001

Schumm, S. (1956). Evolution of Drainage Systems and Slopes in Badlands at Perth Amboy, New Jersey. *Geological Society of America Bulletin 67*(5), 597. https://doi.org/10.1130/0016-7606(1956)67[597:eodsas]2.0.co;2

Sheshukov, A.Y., Sekaluvu, L., Hutchinson, S.L. (2018). Accuracy of topographic index models at identifying ephemeral gully trajectories on agricultural fields. *Geomorphology 306*, 224-234. https://doi.org/10.1016/j.geomorph.2018.01.026

Singh, S., Dubey, A. (1994). *Geoenvironmental Planning of Watersheds in India*. Chugh Publications, Allahabad.

Sørensen, R., Seibert, J. (2007). Effects of DEM resolution on the calculation of topographical indices: TWI and its components. *Journal of Hydrology 347*(1-2), 79-89. https://doi.org/10.1016/j.jhydrol.2007.09.001

Srinivasa Vittala, S., Govindaiah, S., Honne Gowda, H. (2004). Morphometric analysis of sub-watersheds in the pavagada area of Tumkur district, South India using remote sensing and gis techniques. *Journal of the Indian Society of Remote Sensing 32*(4), 351-362. https://doi.org/10.1007/BF03030860

Strahler, A.N. (1952a). Dynamic Basis of Geomorphology. *Geological Society of America Bulletin 63*(9), 923. https://doi.org/10.1130/0016-7606(1952)63[923:DBOG]2.0.CO;2

Strahler, A.N. (1952b). Hypsometric (Area-Altitude) Analysis of Erosional Topography. *Geological Society of America Bulletin 63*(11), 1117. https://doi.org/10.1130/0016-7606(1952)63[1117:HAAOET]2.0.CO;2

Strahler, A.N. (1957). Quantitative analysis of watershed geomorphology. *Eos, Transactions American Geophysical Union 38*(6), 913-920. https://doi.org/10.1029/TR038i006p00913

Strahler, A.N. (1964). *Quantitative geomorphology of drainage basin and channel networks*. In V.T. Chow (ed.), *Handbook of Applied Hydrology* (pp. 4-39 a 4-76). McGraw-Hill.

Tribak, A. (1998). Fonctionnement actuel d'une ravine d'érosion dans une zone de marnes miocènes (région de Tarmast, Prérif oriental, Maroc). Modèle d'évolution et distribution saisonnière des processus. *Revue de géographie alpine 86*(3) 37-48. https://doi.org/10.3406/rga.1998.2890

Tribak, A. (2020). Erosion and Flooding Risks in the Marly Basins of the Eastern Prerif Mountains (Morocco): A Response to Exceptional Climate Events or to Anthropogenic Pressure. *Revista de Estudios Andaluces 40*, 159-182. https://doi.org/10.12795/rea.2020.i40.09

Tribak, A., Baena-Escudero, R., Guerrero-Amador, I.C., Amhani, Z., Abahrour, M., El Garouani, A., Arari, K. (2021). Evaluación de los usos del suelo y la erosión hídrica en la subcuenca hidrográfica montañosa del Oued Ourtza (Pre-Rif Oriental, Marruecos). *Investigaciones Geográficas 76*, 309. https://doi.org/10.14198/INGEO.18851

Vandekerckhove, L., Poesen, J., Oostwoud Wijdenes, D., Gyssels, G., Beuselinck, L., De Luna, E. (2000). Characteristics and controlling factors of bank gullies in two semi-arid mediterranean environments. *Geomorphology 33*(1-2), 37-58. https://doi.org/10.1016/S0169-555X(99)00109-9

Vijith, H., Satheesh, R. (2006). GIS based morphometric analysis of two major upland sub-watersheds of meenachil river in Kerala. *Journal of the Indian Society of Remote Sensing 34*(2), 181-185. https://doi.org/10.1007/BF02991823

Wäldchen, J., Mäder, P. (2018). Machine learning for image based species identification. *Methods in Ecology and Evolution 9*(11), 2216-2225. https://doi.org/10.1111/2041-210X.13075

Weisrock, A. (1980). *Géomorphologie et paléoenvironnement de l'Atlas Atlantique (Maroc)* [Thèse de doctorat d'Etat]. Paris I.

Weisrock, A. (1985). Originalité karstique de l'Atlas atlantique marocain. *Karstologia : revue de karstologie et de spéléologie physique 5*(1), 29-38. https://doi.org/10.3406/karst.1985.2086

Weisrock, A. (2012). Late-middle Pleistocene, late Pleistocene and Holocene palaeo-sea-level records at Agadir and the Atlantic Atlas coastal reach, Morocco: An updated overview. *Quaternaire 23*, 211-225. https://doi.org/10.4000/quaternaire.6252

Weisrock, A., Boudad, L., Ouammou, A., Mhamed, B., Ali, A.H., Chakir, L. (2017). *Quaternary of the semi-arid Moroccan area Field-trip Guide of the 2010 AFEQ-AMEQ*. https://doi.org/10.13140/RG.2.2.35300.27529

Wilson, J., Lorang, M.S. (2000). Spatial models of soil erosion and GIS. In A.S. Fotheringham, M. Wegener (eds.), *Spatial Models Aial and New Models* (vol. 7, p. 83-108). Taylor and Francis.

Xu, Q., Kou, P., Wang, C., Yunus, A.P., Xu, J., Peng, S., He, C. (2019). Evaluation of gully head retreat and fill rates based on high-resolution satellite images in the loess region of China. *Environmental Earth Sciences 78*(15), 465. https://doi.org/10.1007/s12665-019-8483-x

Yang, X., Dai, W., Tang, G., Li, M. (2017). Deriving Ephemeral Gullies from VHR Image in Loess Hilly Areas through Directional Edge Detection. *ISPRS International Journal of Geo-Information 6*(11), 371. https://doi.org/10.3390/ijgi6110371

Zare, M., Soufi, M., Nejabat, M., Pourghasemi, H.R. (2022). The topographic threshold of gully erosion and contributing factors. *Natural Hazards 112*(3), 2013-2035. https://doi.org/10.1007/s11069-022-05254-6